REVIEW

POSS Nanostructures in Catalysis

Carla Calabrese,[a] Carmela Aprile,[b] Michelangelo Gruttadauria*[a] and Francesco Giacalone *[a]

Received 00th January 20xx,
Accepted 00th January 20xx

DOI: 10.1039/x0xx00000x

Polyhedral oligomeric silsesquioxanes (POSS) are organic-inorganic hybrid molecules piquing the research interest thanks to their synergistic features. The great versatility of POSS nanostructures arises from the easy tunability of peripheral organic moieties combined with the high thermal and chemical stability of the inner inorganic core. In this Review, we highlight the use of POSS nanostructures as molecular precursors for the synthesis of homogeneous and heterogeneous catalysts able to promote many processes including alkene epoxidation, C–C bond formation, CO_2 conversion, click reactions, hydrogenations, ethylene polymerization, among others. In this scenario, POSS units found application as molecular model for single-site heterogeneous catalysts, stabilizing platform for metal nanoparticles, metal ligands, supports for organic salts, and molecular buiding blocks for the design of ionic polymers. Herein, we address the catalytic application of POSS nanostructures with the purpose of encouraging the development of performing hybrid catalysts with tailored properties.

Introduction

The chemistry of polyhedral oligomeric silsesquioxanes (POSS) is impacting upon several research fields including material science, nanomedicine, optics, electrochemistry, and catalysis.[1-4] Strictly speaking, POSS are cage-like hybrid molecules described by the general formula $(RSiO_{1.5})_n$ where R is hydrogen or an organic functional group (e.g. alkyl, aryl, alkoxy, alkenyl, siloxy, etc.). In this context, POSS nanostructures with a cubic siloxane core (T_8R_8) represent the most investigated derivative (**Fig. 1**). The synthesis of the simplest cubic POSS (T_8H_8) dates back to 1959 by Müller and co-workers.[5] However, the interest toward this class of molecular hybrids had a progressive growth since the late 1990s. The main synthetic strategy of POSS nanostructures lies in the hydrolytic condensation of organosilanes as trifunctional silicon monomers $RSiX_3$ (where X is usually a halide or alkoxide group). Furthermore, novel derivatives can be prepared by the corner capping of partially condensed silsesquioxanes $T_7R_7(OH)_3$, or the chemical modification of the functional groups of an already existing T_8 core.[6] Based on the nature of the R-functionalities, cubic POSS have a size in the range 1-2 nm and an inner Si–Si diameter of approximately 0.5 nm. The synergistic properties arising from organic and inorganic domains are what makes POSS chemistry a fascinating research topic. The growing interest on POSS nanohybrids is related to the easy tuneability of the organic peripheries combined with their symmetry and the high chemical, thermal and mechanical stability of the inorganic core. On these grounds, POSS molecular structures can be easily modulated to get a broad spectrum of properties including their solubility in many organic solvents. For instance, POSS are excellent nano-sized 3D building block for the design of functional materials.[7-10] They found application as nanofiller in polymers improving thermal and mechanical properties of the resulting nanocomposite.[11-15] The incorporation of these nanostructures as flame retardants allows reducing the flammability of the obtained material as proven by the formation of silicon dioxide on heating.[16] POSS have been used in organic optoelectronic materials and devices, including organic light-emitting diodes (OLEDs), liquid crystal display, sensors and electrochromic devices.[17] Owing to their biocompatibility POSS have been studied as drug carriers, in tissue engineering, and employed for the construction of biomedical devices.[18-21] POSS nanostructures have been applied in the environmental remediation for the preparation of adsorbent materials able to remove inorganic heavy metal ions and organic dyes from wastewater.[22-28] In the field of catalysis, POSS-based hybrids found applications in many processes which will be dealt in this contribution as oxidation reactions, C–C bond formation, polymerization of alkenes, CO_2 conversion, click reactions, and reduction reactions. As depicted in **Fig. 1**, the catalytic active sites can be included in POSS based hybrids by using different strategies. Among them, a selected metal centre can be directly inserted into the POSS inorganic framework through the capping of partially condensed silsesquioxanes $T_7R_7(OH)_3$. Otherwise, the organic moieties of cubic POSS can be post-functionalized to obtain a rich pool of nanohybrids by using conventional organic synthesis methodologies such as substitution reactions, metathesis reactions of POSS-alkenes, and addition reactions. POSS molecules can be modified in order to get task-specific species able to host metal sites as complexes. In this context, POSS nanocages can be modified with specific organic ligands as Schiff bases or phosphines, by construction of dendrimer networks, or by using polymer matrices or organic salts as

[a] Department of Biological, Chemical and Pharmaceutical Sciences and Technologies, University of Palermo, Viale delle Scienze, Ed. 17, 90128, Palermo (Italy).
[b] Department of Chemistry, University of Namur, 61 rue de Bruxelles 5000, Namur (Belgium)

stabilizing platforms for metal nanoparticles (MNPs). POSS organometallic complexes have been also examined as molecular models for silica- and zeolites-grafted catalytic centres. As claimed by Quadrelli *et al.*,[29] the achievement of a structure-activity relationship for heterogeneous catalysts is of paramount importance to improve the catalytic performances or to predict new catalytic reactions. In this context, POSS played a key role to gain better molecular-level understanding of surface reactions and catalysts activity.[29-33] Metal-free POSS nanostructures have been designed and used as organocatalysts for asymmetric Michael addition reactions and for the synthesis of cyclic carbonates from CO_2 and epoxides (*vide infra*). Their nanosized structure combined with eight tuneable organic arms as active sites make POSS molecules promising candidates for catalytic applications for enabling the confined localization of reactants within high concentration of catalytic sites. POSS skeletons have been used for the preparation of both homogeneous and heterogeneous catalytic materials. In particular, several examples of POSS-based heterogeneous catalysts will be discussed including polymeric ionic porous networks and POSS units grafted onto selected solid supports as amorphous or mesostructured silica.

This contribution aims to provide a comprehensive overview on the use of POSS nanohybrids in the vibrant field of catalysis including the most recent literature.

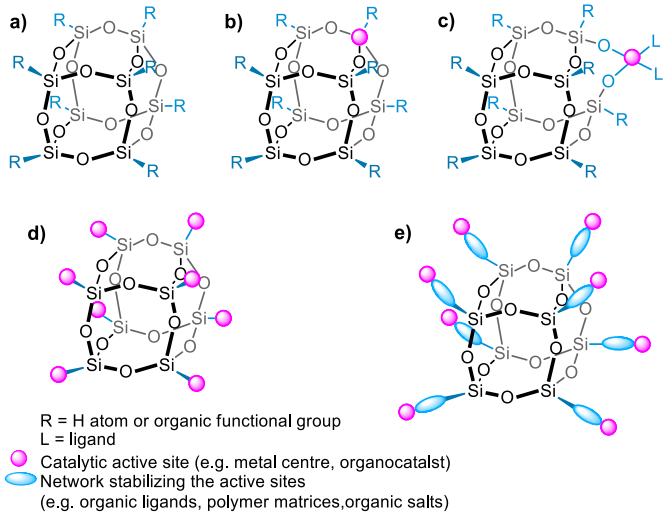

Fig. 1 Functionalized POSS nanocages.

Oxidation Reactions

Oxidation of hydrocarbons

The photo-assisted oxidation of hydrocarbons represents one the first processes related to the use of POSS as nanocatalysts. Mitsudo reported vanadium containing POSS nanocage **1** for the catalytic oxidation of benzene, cyclohexane, and adamantane, under O_2 (1 atm) at around 300 K (**Scheme 1**).[34, 35] POSS catalyst **1** showed higher activity when compared to the homogeneous complex $VO(acac)_2$ suggesting the potential applicability of POSS structures as catalytic support for metal active sites. In a further study, the same research group used vanadium based silsesquioxanes **1** as molecular precursor for silica based heterogeneous catalysts for the photo-assisted oxidation of methane.[36] The synthesis of these materials was performed by wetness impregnation of POSS **1** on silica, followed by air-flow pyrolysis at 523 or 723 K. The thermal treatment at higher temperatures led to a heterogeneous catalyst for the photooxidation of methane into formaldehyde with improved performance than that of a silica supported vanadium reference catalyst. The possibility of using POSS nanostructures as molecular precursor for porous oxide materials was prompted also by the specific textural properties of the final catalyst as the high surface area (349 m^2g^{-1}) and more mesopores with a size around 3 nm than the parent silica support.

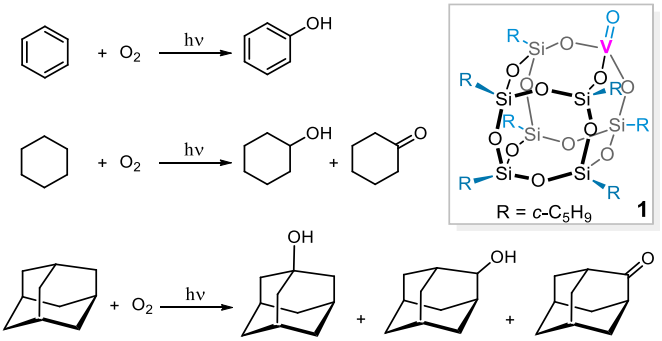

Scheme 1 Photo-assisted oxidation of hydrocarbons catalyzed by V-POSS **1**.

More recently, the oxidation of hydrocarbons has been catalyzed by POSS-based porous cationic frameworks **3** developed by Chen *et al.* (**Scheme 2**).[37] Catalyst **3** was prepared starting from the quaternization between octakis(chloromethyl)POSS **2** monomer and 4,4'-bipyridine as organic linkers. The obtained ionic frameworks were used as solid support for POM species $[PMo_{10}V_2O_{40}]^{5-}$ through anionic exchange to give the final material **3**. The catalytic performance was evaluated in the aerobic hydroxylation of benzene to phenol with molecular oxygen as the oxidant and ascorbic acid as reducing agent, at 100 °C. After 10 h of reaction, phenol was obtained with 12% yield corresponding to a catalytic turnover number (TON) of 136 based on the content of heteropolyanion $[PMo_{10}V_2O_{40}]^{5-}$. Under homogeneous reaction conditions, the equivalent $[PMo_{10}V_2O_{40}]^{5-}$ led to a much lower phenol yield of (4.6%) than catalyst **3**. The catalytic activity of **3** was related to its peculiar morphology characterized by narrow distributed mesopores and a high surface area enabling the dispersion and the accessibility of the active $[PMo_{10}V_2O_{40}]^{5-}$ sites. The presence of hydrophobic POSS units could improve the compatibility of the catalyst to hydrophobic organic substrates, promoting the rapid adsorption of benzene and timely release of phenol. Furthermore, the authors argued that π-extended viologen cations could influence the electronic state of $[PMo_{10}V_2O_{40}]^{5-}$ stabilizing the reduced V^{4+} state which activate O_2 to create the active oxygen species allowing the formation of the final product. The oxidation of the less reactive cyclohexane to cyclohexanol and cyclohexanone was carried out in the presence of H_2O_2 at 80 °C for 6 h. Catalyst **3** gave rise to

cyclohexanone with a yield of 32.2% and turnover number of 2,439. In this process **3** was reused three times without significant loss of activity (down to 28.8% of yield and TON of 2,182). In this case as well, the achieved yield and TON values were higher than those reported from the equivalent pure $[PMo_{10}V_2O_{40}]^{5-}$ homogeneous system (cyclohexanone yield of 27.2% and TON of 2,060).

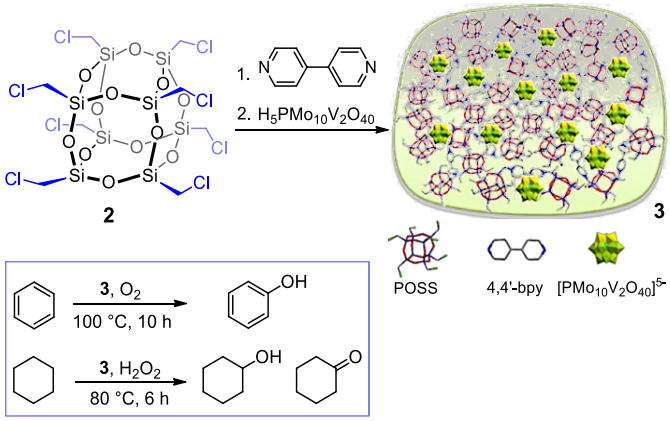

Scheme 2 POSS porous ionic frameworks **3** for the oxidation of hydrocarbons. Adapted from reference 37. Creative Commons Attribution 4.0 International License.

Alkene epoxidation

The epoxidation of alkenes catalyzed by tailored POSS-based nanostructures dates back to 1997 by Abbenhuis and co-workers.[38] The titanium complex **4** (**Scheme 3**), firstly published in 1992,[39] was used as catalyst at 1.4 mol% in the epoxidation of some alkenes with *tert*-butyl hydroperoxide (TBHP) as oxidizing agent at 50 °C. The corresponding epoxides were obtained in high yields (80-90%) with a good selectivity (80-95%). The same research group reported a study on the immobilization of titanium complex **4** on MCM-41.[40] Catalyst **4** was adsorbed into the channels of MCM-41 supports with different Si/Al ratios. The resulting self-assembled materials **5** were used as heterogeneous active catalysts for alkene epoxidation in liquid phase at 50 °C with TBHP. Catalysts **5** showed lower activity when compared with the homogeneous complex **4**. When titanium complex **4** was adsorbed into aluminium-free MCM-41, no catalytic deactivation was observed for the solid. This catalyst was recovered from the reaction by filtration and reused for three times without loss of activity. According to data, the presence of aluminium in MCM-41 reduces the activity of the catalyst, unless the solids were treated with a silylating agent as $SiCl_2Ph_2$ prior to catalysis. As claimed by the authors, the good adsorption of catalyst **4** is strictly influenced also by the mesoporous morphology of the solid support.[41] When complex **4** was immobilized on conventional silica gel a significant catalyst leaching was observed during the catalytic tests.

The tripodal Ti-POSS complexes **6-9** reported in **Fig. 2** were prepared from incompletely condensed silsesquioxanes with homoleptic titanium(iv) complexes to be tested as homogeneous catalyst in the epoxidation of 1-octene with TBHP at 80 °C.[42]

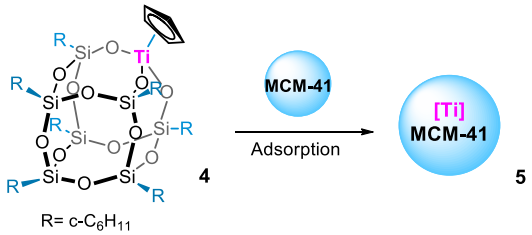

Scheme 3 Titanium-POSS complex **4** and its adsorption into MCM-41 (**5**) for epoxidation reactions.

These complexes proved to be more active than complexes with lower number of coordination to siloxy groups. Few years later, the application of high-speed experimentation techniques with a broad screening of reaction parameters allowed optimizing the time-consuming synthesis of several silsesquioxane precursors for titanium catalysts active in the epoxidation of alkenes with peroxides.[43, 44] The catalytic performance of homogeneous POSS molecules bearing titanium as single site encouraged the research toward the design of heterogeneous catalysts based on Ti-POSS units.

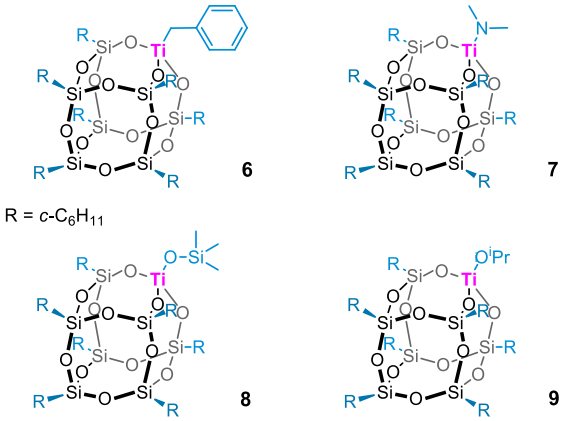

Fig. 2 Ti-POSS complexes **6-9** for the epoxidation of alkenes.

Scheme 4 provides a further example of supported Ti-POSS nanostructures. Titanium silsesquioxanes complexes **10a-b** were grafted on commercially available linear methylhydrosiloxane-dimethylsiloxane copolymers (HMS-301) and then cross-linked by reaction with vinyl-terminated polydimethylsiloxanes (DMS-V05).[45] The obtained titanium polysiloxane materials **11a-b** were used in the epoxidation of cyclooctene with equimolar amounts of TBHP (0.33 mol% Ti, 50 °C, 24 h). Under these reaction conditions, **11a** and **11b** showed selectivity >95% with 73% and 55% conversion into cyclooctene epoxide, respectively. Then, the catalytic activity of **11a** and **11b** was tested in the epoxidation of cyclooctene with 35% aqueous hydrogen peroxide (0.33 mol% Ti, 50 °C, 24 h) being **11b** more active than **11a**. The performances of **11b** were investigated with n-alkenes and large cyclic alkenes by using H_2O_2 as oxidizing agent. In particular, the catalytic epoxidation of 1-octene with **11b** was optimized to give the corresponding epoxide in 62% yield in 1.5 h (2 mol% Ti, 80 °C).

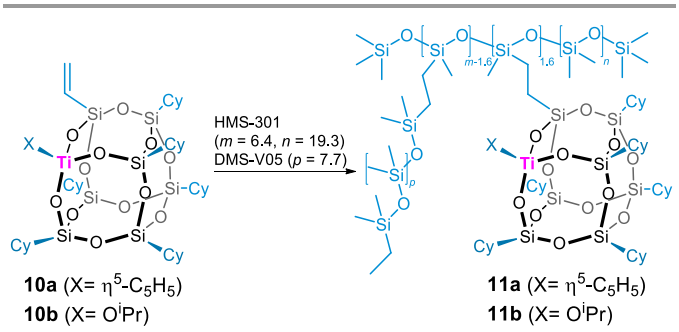

Scheme 4 Ti-POSS catalysts (**10a-b**) supported on polysiloxanes (**11a-b**).

Heterogeneous catalysts based on Ti-POSS units for the epoxidation of alkenes were reported in 2007 by Li *et al*..[46] Homogeneous Ti-POSS complexes were immobilized by *in situ* copolymerization on a mesoporous SBA-15 supported polystyrene polymer (**Fig. 3**). The resulting hybrid materials exhibit attractive textural properties (highly ordered mesostructure, large specific surface area (> 380 $m^2\ g^{-1}$) and pore volume ≥ 0.46 $cm^3 g^{-1}$. In the epoxidation of cyclooctene with TBHP at 60°C, hybrid catalysts **12** had rate constants comparable with that of their homogeneous counterpart. The recyclability of this type of material was investigated for seven reuses showing a low decrease in the catalytic activity (from 88% to 77% of epoxide yield). The epoxidation of cyclooctene was performed also with aqueous H_2O_2 as the oxidant at 60 °C. In two-phase reaction media, these catalysts showed much higher yields (>25%) than their homogeneous counterpart (8.4% of epoxide yield). This behavior was attributed to the hydrophobic environment nearby Ti active sites in the heterogeneous hybrids. As claimed by the authors, the Ti-POSS compound may suffer irreversible hydrolysis of its siloxy-titanium bonds in aqueous H_2O_2. The inactivity of both homogeneous Ti-POSS and the physically adsorbed Ti-POSS in MCM-41 was thus explained for epoxidation processes carried out with aqueous H_2O_2. It was assumed that the polymer around Ti-POSS units provide protection of titanium active sites against hydrolysis by water.

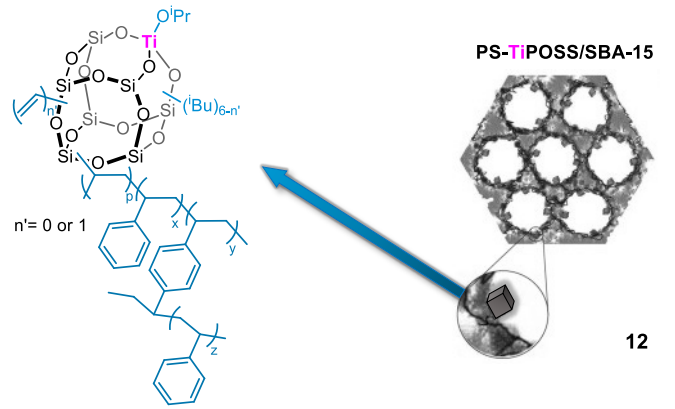

Fig. 3 PS-TiPOSS/SBA-15 **12** as catalyst for the epoxidation of alkenes. Adapted from Ref. 46. Copyright 2007, WILEY-VCH Verlag GmbH & Co. KGaA, Weinheim.

In order to evaluate the influence of POSS nanocages, two reference titanium containing silica materials were prepared by grafting $Ti(Cp)_2Cl_2$ precursors onto mesoporous silica supports (Ti/SBA-15, Ti/SiO_2-Dav). The catalytic tests were carried out using TBHP at 85 °C for 24 h. In the epoxidation of limonene supported Ti-POSS **13** units led to lower conversions with respect to reference materials (Ti/SBA-15 or Ti/SiO_2-Dav). However, in terms of selectivity, the anchored Ti-POSS materials displayed slightly better results than those obtained over reference Ti-silica catalysts. In all cases, the endocyclic limonene epoxide was obtained with selectivity values in the range 80-88%. In the epoxidation of carveol, turnover frequency values (TOF calculated as $mol_{converted\ alkene}/mol_{Ti}{\cdot}h^{-1}$) of supported Ti-POSS **13** materials (1.96-2.17 h^{-1}) were almost the same of reference catalyst Ti/SBA-15 (2 h^{-1}). However, supported Ti-POSS **13** materials showed a higher selectivity to endocyclic epoxide than titanocene-derived systems (ca. 80% *vs.* 60%, respectively). Supported dinuclear dimer Ti-POSS **14** species were tested in the epoxidation of limonene, carveol, and α-pinene. In this case as well, Ti-POSS **14** grafted onto mesoporous silicas showed, on average, a lower catalytic activity in terms of TOF and slightly higher selectivity by comparison with reference Ti-silica solids. The better selectivity to endocyclic epoxides of supported Ti-POSS **13-14** materials was ascribed to a more marked acidic character of reference titanocene modified silicas related to the formation of undesired acid catalyzed secondary products.

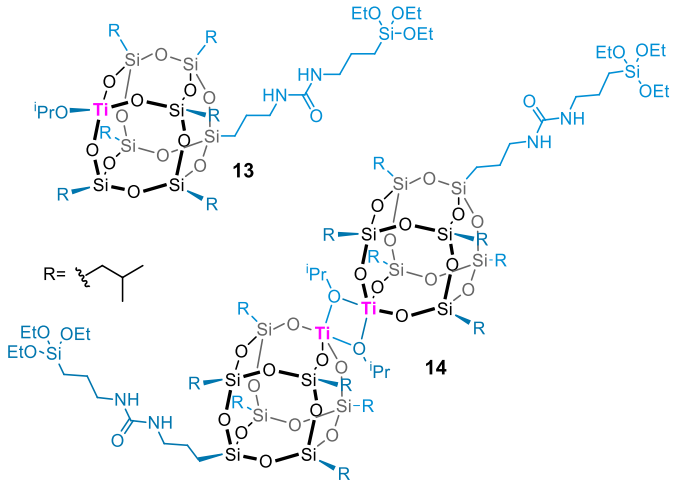

Fig. 4 Ti-POSS complexes **13**-**14** for the design of siliceous heterogeneous catalyst.

Wada and co-workers reported a series of silica supported titanium oxide heterogeneous catalysts for the epoxidation of cyclooctene and limonene with TBHP.[49] Such materials were prepared by the calcination of Ti-bridged POSS with four Si–O–Ti bonds, $Ti[(c\text{-}C_5H_9)_7Si_7O_{11}(OSiMe_2R)]_2$ and $Ti[(c\text{-}C_5H_9)_8Si_8O_{13})]_2$ previously impregnated onto several silica supports. The catalytic tests were run at 0.5 mol% of Ti, in a toluene solution of alkene at 60 °C in 4 h. Cyclooctene oxide was selectively obtained with yields in the range of 66-88% corresponding to TOF values of 33-44 h^{-1}. A corner capped Ti-POSS, $CpTi[(c\text{-}C_5H_9)_7Si_7O_{12})]$ and tetraisopropoxytitanium were used for the synthesis of silica supported catalysts. However, the obtained solids displayed lower catalytic performances by comparison with silica supported Ti-bridged POSS units. A few year later, Wada *et al.* deepened the use of the same Ti bridged

silsesquioxanes as catalytic frameworks for the design of silica based heterogeneous catalysts for the epoxidation of cyclooctene.[50]

In 2009, Ti-containing silsesquioxane gel catalysts were prepared by the hydrosilylative condensation of Ti-silsesquioxanes together with cubic silsesquioxanes and spherosilicates. The porosity of gels was tuned by changing the composition and the mixing order of the starting materials. Both porous and nonporous gels were able to catalyze the selective epoxidation of cyclooctene by using of aqueous hydrogen peroxide as the oxidant, in toluene at 60 °C.[51] In 2010, tripodal titanium-silsesquioxanes complexes were encapsulated in a polydimethylsiloxane membrane (PDMS) to be used as heterogeneous catalysts in the epoxidation of cyclohexene and 1-octene with aqueous H_2O_2 (**Scheme 5**).[52] The activity of **15a-b** was studied at 2 mol% of Ti and 60 °C. Acetonitrile was used as solvent for its miscibility with olefins and aqueous H_2O_2 and, at the same time, because it does not swell PDMS to any appreciable extent. Cyclohexene oxide and 1,2-epoxyoctane were obtained with high selectivity and excellent H_2O_2 efficiency. Both **15a** and **15b** were successfully reused in 1-octene epoxidation for five consecutive cycles without showing any decrease in the catalytic performance. It is worth to mention that the unsupported Ti-POSS catalysts showed no activity with H_2O_2. The lack of catalytic activity under homogeneous reaction conditions was probably due to excessive coordination of water to Ti sites of POSS nanocages. As explanation of the efficient use of H_2O_2 by **15a** and **15b**, the authors suggested that PDMS membrane provided a uniformly non-polar environment around Ti-POSS complexes resulting in low local water concentration, as well as higher [alkene]/[H_2O_2] ratios at the Ti center than in the bulk reaction medium.

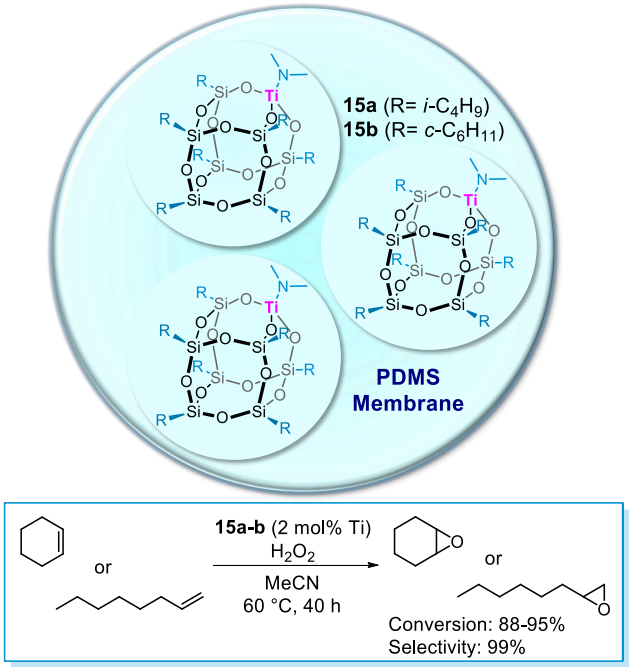

Scheme 5 Ti-POSS complexes **15a-b** encapsulated in PDMS membrane for the epoxidation of alkenes.

In 2013, Filho *et al.* developed the first example of molybdenum complexes immobilized on POSS nanostructures for the epoxidation of alkene (compound **16**, **Fig. 5**).[53] POSS units were modified with 2-amino-1,3,4-thiadiazole moieties to be used as ligand for the complex [Mo(η^3-C_3H_5)Br(CO)$_2$(NCMe)$_2$]. The activity of Mo-POSS molecular hybrid **16** was investigated in the epoxidation of cyclooctene and styrene by using TBHP as oxidant, in dichloromethane as solvent, at 55 °C for 24 h. Catalysts **16** was tested at 1 mol% showing TOF values of 147 and 90 h^{-1} for the epoxidation of cyclooctene and styrene, respectively. In 2015 Calhorda *et al.* reported POSS supported Mo complex together with a series of materials based on analogous Mo complexes, such as **16**, immobilized onto MCM-41 and silica gel.[54] In the oxidation of 1-octene with TBHP, Mo-POSS complex displayed significantly better activity than both the unsupported analogous and silica supported molybdenum complexes. In this process, POSS-based molybdenum systems showed high selectivity toward the epoxide (>99%) and a TOF value after 10 minutes of reaction of 66 h^{-1}. The better performance of a POSS-based catalyst was related to the nature of the nanocaged support leading to improved access to the metal center without significant steric restraints. The preliminary study of Fihlo was followed by the synthesis of Mo-POSS complexes **17** and **18** prepared by reaction of POSS units bearing 3-amino-1,2,4-triazole-5-carboxylic acid moieties with [Mo(η^3-C_3H_5)Br(CO)$_2$(NCMe)$_2$] or [Mo(CO)$_3$Br$_2$(NCMe)$_2$].[55] Hybrids **17** and **18** were tested at 1 mol% as heterogeneous catalysts in the epoxidation of six olefins with TBHP at 55 °C in dichloromethane.

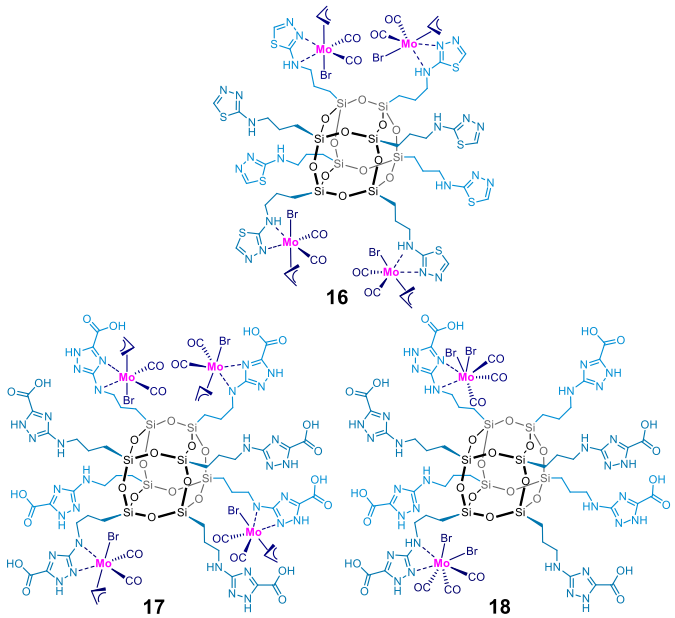

Fig. 5 Mo-POSS complexes **16**-**18** for the epoxidation of alkenes.

Catalyst **17** proved to be more active than **18** showing high TOF values in the range 129-166 h^{-1} and similar performance with respect to homogeneous molybdenum complexes. In another study, the same authors supported [W(CO)$_3$Br$_2$(NCMe)$_2$] complex on the same POSS units used for the synthesis of catalysts **17** and **18**.[56] The obtained tungsten hybrids (W-POSS)

showed slightly lower performance with respect to the homogeneous complex. Under the same reaction conditions, W-POSS exhibited higher activity than Mo-POSS **18** and worst performance by comparison with Mo-POSS **17**. Furthermore, Filho *et al* used POSS molecule with aminopropyl functionalities as the core of polyamidoamine dendrimers for the design of supported molybdenum complexes catalysts.[57] Molybdenum complexes $[Mo(\eta^3\text{-}C_3H_5)Br(CO)_2(NCMe)_2]$ and $[Mo(CO)_3Br_2(NCMe)_2]$ were fixed onto a second generation POSS dendrimer to give novel heterogeneous catalysts for the epoxidation of alkenes with TBHP. The catalytic tests were run in dichloromethane as solvent, at 55 °C for 24 h. The most active metallodendritic catalyst, based on POSS supported $[Mo(\eta^3\text{-}C_3H_5)Br(CO)_2(NCMe)_2]$ complex, was used at 1 mol% for the epoxidation of six alkenes with conversion between 76-97% corresponding to TOF values in the range 180-260 h^{-1}. One year later, in 2017, Filho *et al* used the same second generation POSS dendrimer to immobilize $[W(CO)_3Br_2(NCMe)_2]$ complex.[58] However, under the same reaction conditions, tungsten dendritic POSS catalyst showed lower activity in terms of TOF values (47-118 h^{-1}) when compared to the above mentioned molybdenum supported dendritic catalysts.

Octa(3-aminopropyl) POSS **19** was used as building block for immobilizing the oxo-molybdenum Schiff **20** previously treated with $SOCl_2$ (**Scheme 6**).[59] The prepared POSS-bridged oxo-molybdenum complex **21** catalyzed the epoxidation of alkenes with TBHP as the oxidant, in CH_3Cl at 70 °C. Cyclooctene was selected as starting olefin to compare the catalytic activity of the heterogeneous hybrid **21** with its homogeneous analogues **20** and $MoO_2(acac)_2$.

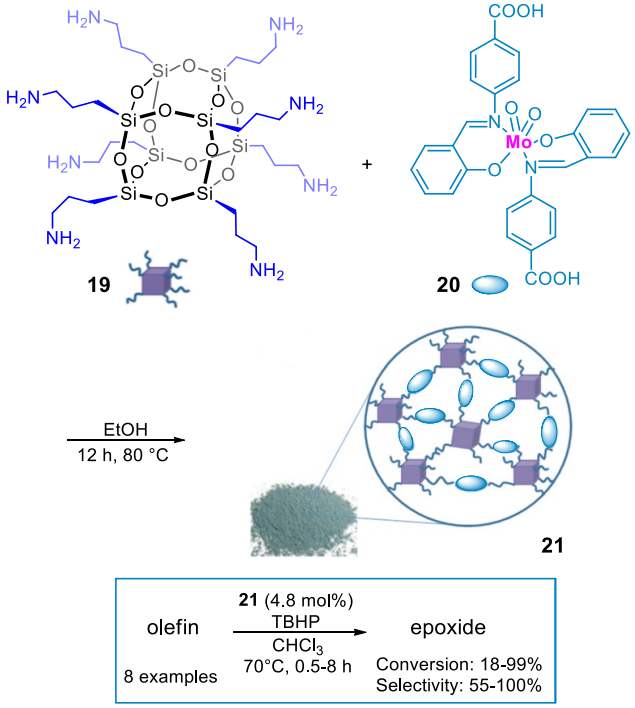

Scheme 6 POSS-bridged oxo-molybdenum Schiff base complex **21**. Adapted from Ref. 59 with permission from The Royal Society of Chemistry.

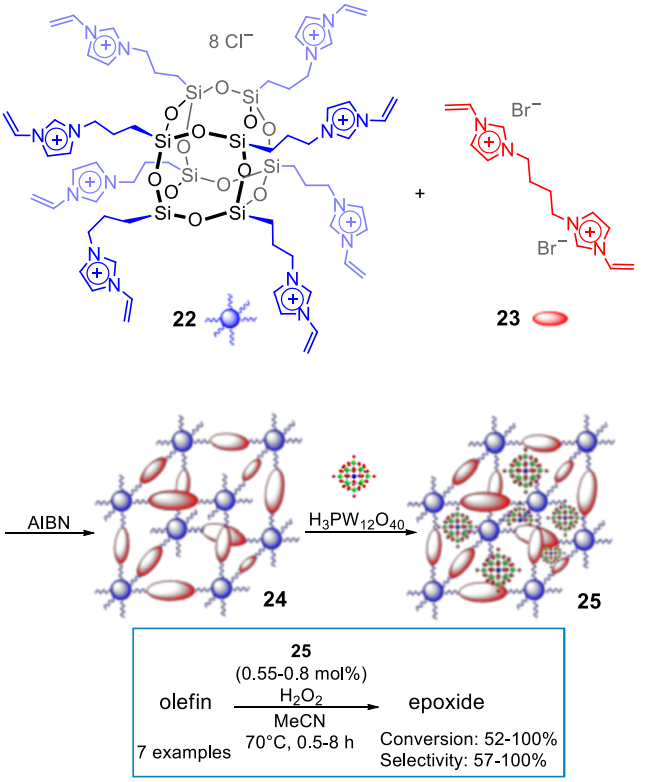

Scheme 7 Synthesis of POM ionic hybrids **25** using POSS units as building blocks. Adapted from Ref 60. Copyright 2014, American Chemical Society.

According to their results, **21** exhibited a much higher activity than its homogenous counterparts **20** and $MoO_2(acac)_2$. The enhanced catalytic activity of **21** was attributed to the hydrophobic core of POSS nanostructures. As testified by contact angle measurements, both TBHP and olefins had a good wettability on **21** which was able to supply a more accessible microenvironment for the reactants toward Mo active sites. A broad scope of aromatic and aliphatic alkenes was tested with catalyst **21** showing TOF values up to 41 h^{-1}.

Leng *et al.* developed polymeric hybrids based on cross-linked POSS nanocages bearing imidazolium moieties as support for polyoxometalate (POM) active species.[60] The free radical copolymerization of vinylimidazolium modified POSS **22** and bis-vinyl imidazolium salt **23** allowed to a series of hybrids **24** which were in turn reacted with $H_3PW_{12}O_{40}$ to obtain suitable materials for the epoxidation of alkenes (**Scheme 7**). The catalytic performances of the polyoxometalate-based ionic hybrids **25** were assessed by using cyclooctene as probe substrate, aqueous H_2O_2 as oxidant, and acetonitrile as solvent at 70 °C for 6 h. Collected data evidenced how the catalytic performance were influenced by the molar ratio of the dicationic organic salt with POSS units. The increase of the molar ratio of the bis-vinyl imidazolium salt to POSS from 2 to 11 led to continuous increase in surface areas (15.6-42 m^2/g), pore volumes (0.06-0.16 cm^3/g), and catalytic activity toward the selective formation of cyclooctene oxide. The mesoporous POM-based ionic hybrid with the molar ratio of the bis-vinyl imidazolium salt to POSS equal to 8 exhibited 100% selectivity with a quantitative conversion into cyclohexene oxide. This catalyst was used with different substrates such as styrene,

cyclohexene, 1-octene, 1-hexene, cis-3-hexenol, and bipentene with good catalytic activities (epoxide conversion 52-92%) and selectivity (57-99%). Considering the epoxidation of cyclooctene, it is worth to mention that the homogeneous $H_3PW_{12}O_{40}$ only gave a 26% conversion and 81% selectivity. The low selectivity is ascribed to the strong acidity of $H_3PW_{12}O_{40}$ leading to the ring-opening and deep oxidation of the epoxidation product. The POSS-free counterpart based on cross-linked imidazolium-POM networks also exhibited a low conversion of 42%. The above comparisons evidences that POSS units are indispensable for the high activities of the target POM catalyst for the epoxidation of cyclooctene with H_2O_2.

In 2015 the same group reported an amphiphilic POM catalytic systems prepared by the copolymerization of octavinyl-POSS, [3-dodecyl-1-vinylimidazolium] bromide, and [3-propionic acid-1-vinylimidazolium] bromide followed by ion exchange with the $[PO_4(WO_3)_4]^{3-}$ species.[61] The catalytic activity and reusability was tested in the epoxidation of cyclooctene using H_2O_2. Cyclooctene oxide was obtained with full selectivity and quantitative conversion. The amphiphilic catalyst was employed also with several substrates such as cyclohexene, 1-octene, 1-hexene, and cis-3-hexenol reporting conversion in the range 49-99% and selectivity >94%. Focusing on this research topic, Len *et al.* proposed a further series of heterogeneous catalyst for the epoxidation of several alkenes.[62] Octavinyl-POSS **26** and imidazolium salts bearing hydrophobic alkyl chains with different lengths were used as building blocks for the synthesis amphiphilic POM hybrids **27** *via* free radical polymerization and ion exchange reactions (**Scheme 8**). By varying the molar ratio of the imidazolium salt to POSS and the imidazolium alkyl side chain, a series of ionic copolymers with different textural properties were proposed. The obtained hybrids were found to be efficient catalysts for the epoxidation of cyclooctene with H_2O_2 as the oxidant, in acetonitrile as solvent at 70 °C in 2 h. A selected catalyst was tested with several alkenes and reused for five runs without observing loss in catalytic activity.

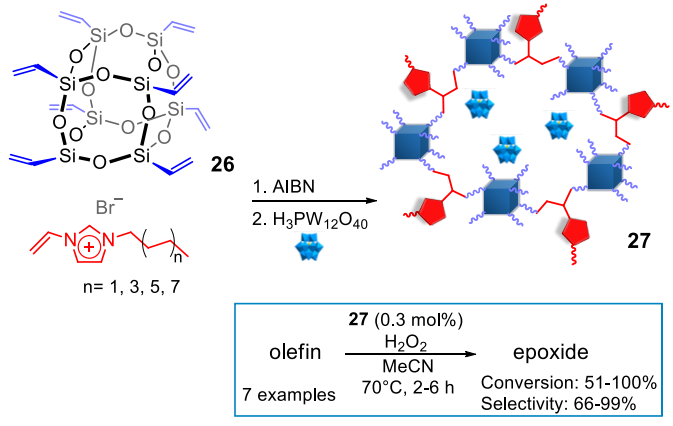

Scheme 8 POSS ionic hybrid polymers **27** as catalysts for alkene epoxidations.

Recently, tantalum-POSS complexes **28** and **29** were synthesized and examined as catalysts for epoxidations with aqueous hydrogen peroxide (**Fig. 6**).[32] Ta-POSS complexes were used to model silica-bound Ta sites and showed to be active in the epoxidation of cyclooctene. Compound **28** with one Ta center and two $-OSi(O^tBu)_3$ ligands, decomposed after a few catalytic cycles into an inactive new complex with two POSS ligands. A similar process might be possible on the silica surface, leading to deactivation of a supported catalyst. A lower loss of activity from 90% to 76% of epoxide yield was observed after three catalytic runs of **29**. By comparison with **28**, the presence of μ-oxo and μ-hydroxo bridges, and perhaps the germanoxy ligands, are possible keys for higher stabilization of Ta in **29** during the catalysis. According to the authors, **28** is the first Ta-POSS complex as efficient catalyst for the epoxidation of cyclooctene using aqueous H_2O_2. Catalyst **29** with cyclooctene as substrate and a catalyst:alkene:H_2O_2 ratio of 1:600:50, led to the same conversion at 65 °C or at room temperature (94%), being the reaction at 65 °C much faster (1 h *vs* 7 h). At room temperature, catalyst **29** with a cyclooctene:H_2O_2 ratio of 1:1 allowed obtaining a 94% conversion in 24 h (catalyst:alkene:H_2O_2 ratio 1:50:50).

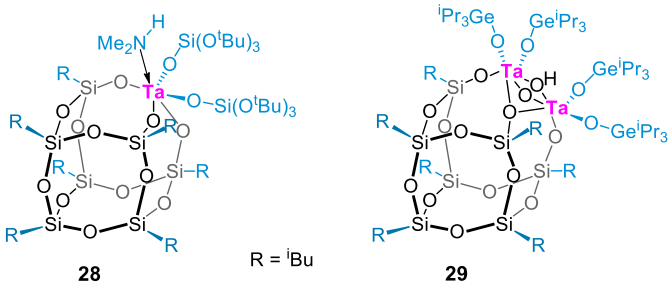

Fig. 6 Ta-POSS **28**-**29** as functional catalysts for epoxidation.

Alcohol oxidations

Wada *et al.* firstly proposed a catalytic system based on pyridine modified POSS **30** as $Pd(OAc)_2$ ligand for the oxidation of alcohols with air or molecular oxygen (**Scheme 9**).[63] The combined use of $Pd(OAc)_2$ and **30** (0.1 mol%) afforded benzaldehyde in 97% yield without the formation of precipitates. On the other hand, the reaction yield decreased from 97% to 86% when $Pd(OAc)_2$ and pyridine were used inducing to the formation of palladium black.

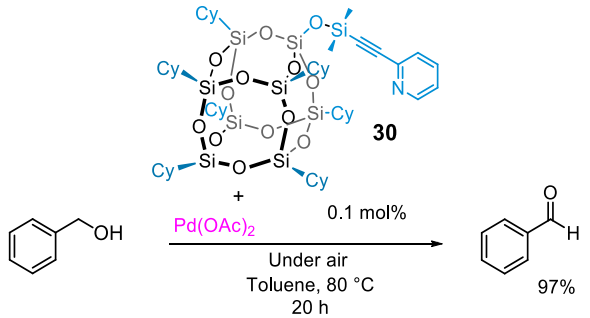

Scheme 9 Benzyl alcohol oxidation catalyzed by $Pd(OAc)_2$ and pyridine-POSS **30**.

In 2017, POSS-based material **31** was prepared *via* free radical polymerization of methyl methacrylate functionalized POSS mixture (T_8, T_{10}, T_{12}) followed by the immobilization of Pd nanoparticles (**Scheme 10**).[64] The resulting hybrid was able to

catalyze at 0.43 mol% the aerobic oxidation of benzyl alcohol to benzaldehyde in quantitative yield using a mixture of a H_2O/Pluronic (P123) solution after 6 h at 90 °C. Several benzyl alcohol derivatives were converted to the corresponding aldehydes in good to excellent yields by using **31**. The substrate scope investigation evidenced that electron-rich benzyl alcohol derivatives were more readily oxidized than the related electron-withdrawing substrates. With benzyl alcohol derivatives featuring electron-withdrawing substituents, high conversions were achieved with 1 equivalent of K_2CO_3 additive and longer reaction times (up to 96 h).

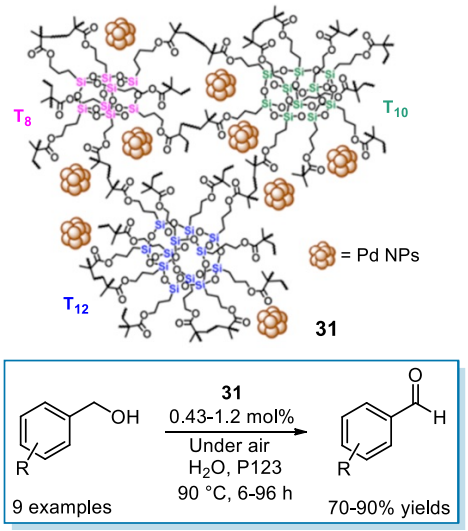

Scheme 10 Pd supported POSS based cross-linked networks **31** for alcohol oxidations. Adapted from Ref. 64. Copyright 2017, American Chemical Society.

More recently, Wang *et al.* reported a series of porous ionic polymers with polyoxometalate anions as support for palladium nanoclusters.[65] The catalysts were prepared starting from the copolymerization between octa-vinylPOSS **26** and 3,3-methylene divinylimidazolium dibromide. Then, several polyoxometalate anions ($[PMo_{12}O_{40}]^{3-}$, $[PW_{12}O_{40}]^{3-}$, $[SiW_{12}O_{40}]^{3-}$) were inserted in the obtained cross-linked networks through anion-exchange. The resulting hybrids were treated with a solution of $Pd(OAc)_2$ to be thereafter reduced by $NaBH_4$ (**Scheme 11**). Catalyst **29** was used at 0.001 mol% of Pd for the solvent free oxidation of benzyl alcohol derivatives with O_2 at 160 °C affording good yields (72-99%) and selectivity values in the 74-99% range.

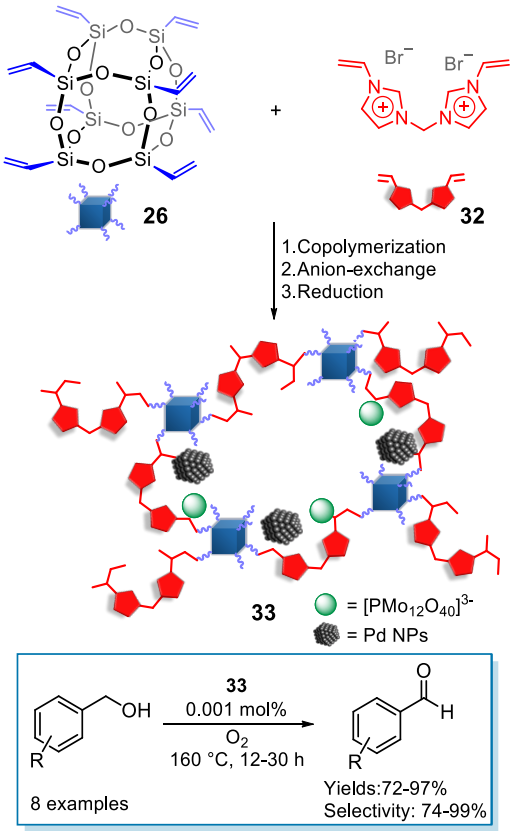

Scheme 11 Pd supported POSS based ionic polymers for alcohol oxidations.

Interestingly, under the same reaction conditions **29** led to the conversion of benzyl alcohol into benzaldehyde with much higher turnover number than commercial Pd/C catalyst (85,683 *vs* 134 respectively). Furthermore, catalyst **29** showed good reusability without showing any significant decrease in performance after four consecutive cycles.

Formic acid electrooxidation

In 2014 octa(3-aminopropyl) POSS **19** was used as capping agent and complexing agent for the synthesis of octahedral Pt-Pd alloy nanoparticles in the presence of methanol as reductant and solvent.[66] The molar amount of **19** represented a key factor for the formation of octahedral Pt-Pd NPs with uniform size and good dispersability. The electrocatalytic activity, CO tolerance and stability of octahedral Pt-Pd NPs were examined with cyclic voltammetry, CO stripping voltammetry and chronoamperometry, respectively (**Fig. 7**). By comparison with Pt nanoparticles and commercial Pt black, the octahedral Pt-Pd NPs showed enhanced electrocatalytic activity, increased CO tolerance and favourable stability for the electrooxidation of formic acid.

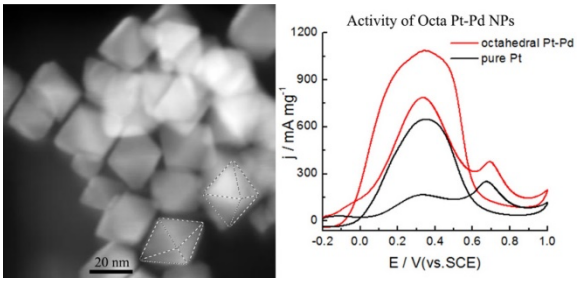

Fig. 7 HRTEM image and CV of octahedral Pt-Pd NPs. Reproduced from Ref. 66. Copyright 2014, Elsevier Ltd.

In 2015, octa(3-aminopropyl) POSS **19** was employed for the synthesis of bimetallic platinum–bismuth nanoparticles (Pt-Bi NPs).[67] These nanoparticles were tested for high-performance electrooxidation of formic acid. Their characterization evidences a homogeneous-phase with blackberry-like morphology when the fraction of Bi was no less than 60%. Their electrocatalytic activity was studied with cyclic voltammetry and chronoamperograms. The prepared bimetallic Pt-BiNPs displayed larger electrochemical surface areas, better electrocatalytic activity and more favourable durability towards electrocatalytic oxidation of formic acid compared with commercial catalysts. As claimed by the authors, such improvement could be ascribed to the role of octa(3-aminopropyl) POSS **19** as the control agent of morphology and the carrier of electrocatalyst with possible corrosive resistance. This study suggested that POSS nanostructures might potentially facilitate preparation of homogeneous-phase nanocatalysts for direct formic acid fuel cells. More recently, Ge and coworkers reported a series of POSS stabilized platinum-palladium alloy nanoparticles with morphology evolution and catalytic activity in the electrooxidation of formic acid.[68] In particular, the Pt-Pd alloy NPs were synthesized in an aqueous solution by simultaneously reducing Pt and Pd precursors with formaldehyde in the presence of octa(3-aminopropyl) POSS **19** as the stabilizer. By varying the ratio of Pt to Pd, the Pt-Pd alloy NPs evolved from truncated octahedrons to octahedrons, and triangular nanoplates (**Fig. 8**). The proposed mechanism of morphology evolution concerned the Pt and Pd self-assembly on POSS to form Pt_xPd_{1-x} intermediates with different Pt/Pd ratios. In addition, formaldehyde could selectively bind to the [111] facets of Pd to control the growth rates of different facets and help Pt_xPd_{1-x} intermediates with different Pt/Pd ratio grow into different morphology of Pt_xPd_{1-x} alloys. The morphology tuning endowed the Pt-Pd alloy NPs good performance in terms of large electrochemically active surface area, high electrocatalytic activity, durability toward oxidation of formic acid, and CO tolerance. The same research group reported the synthesis of well-dispersed Pt-Pd NPs (average particle diameter 6.5 nm) by using octa-maleamic acid silsesquioxanes as the stabilizing agent with hydrothermal method.[69] The best molar ratio of POSS to metal precursors was found to be 1:2, respectively. The obtained well-dispersed Pt-Pd NPs displayed enhanced electrocatalytic performance, stability and tolerance to CO poisoning in formic acid oxidation.

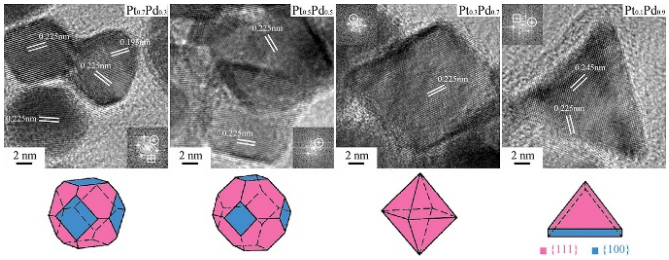

Fig. 8 Morphology evolution of Pt_xPd_{1-x} alloy NPs for formic acid electrooxidation. Reproduced from Ref. 68. Copyright 2017, Elsevier Inc.

Miscellaneous oxidations

In 2004, osmium silsesquioxane complex **34** was synthesized and tested as homogeneous catalyst for the dihydroxylation of olefns.[70] This Os-POSS complex was used also as molecular model of the catalytic site of a silica-supported heterogeneous Os-catalyst. Compound **34** was prepared by complexation of osmium tetroxide with a silsesquioxane ligand containing a tetrasubstituted olefin moiety. The advantage of this procedure lies in avoiding the presence of the highly toxic and volatile OsO_4 in solution during the dihydroxylation reaction. Os-POSS complex **34** was able to catalyze the dihydroxylation of cyclopentene and cyclohexene at room temperature by using *N*-methylmorpholine-*N*-oxide (NMO) as the oxidant. The achieved cyclohexene conversion (99% in 3 h) was higher than that of cyclopentene (84% in 24 h). The different reactivity of the substrates was explained by the fact that the complex between the osmium centre and the cyclopentene ring is geometrically more strained and less favourable than the one involving cyclohexene. The turnover number values of **34**, after 3 h of reaction, were found to be 130 and 414 for the conversion of cyclopentene and cyclohexene, respectively.

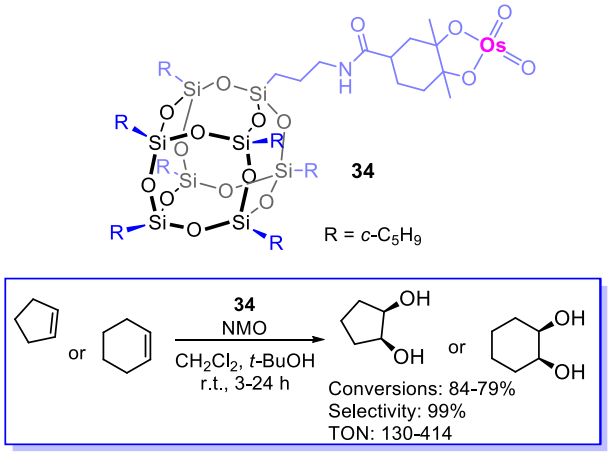

Scheme 12 Os-POSS complex for dihydroxylation reactions.

In 2009, iron (III)-containing POSS compounds **35a-d** were developed and applied as catalysts for the aerobic oxidation of tetrahydrofuran (**Scheme 13**).[71] The major oxidation product was γ-butyrolactone, whereas two minor products were 2-hydroxy-THF and its tautomer, 4-hydroxybutanal. The achieved turnover numbers suggested that smaller substituents on the POSS ligands improved the stability of the catalytic species. The iron (III) chloro-POSS complexes **35a-d** were able to generate

between 74 and 114 equivalents of γ-butyrolactone per mole of iron (III). The much lower turnover numbers displayed by the sole $[Bu_4N][FeCl_4]$ (TON = 6) proved the stabilizing role of POSS ligands towards the catalytic active sites.

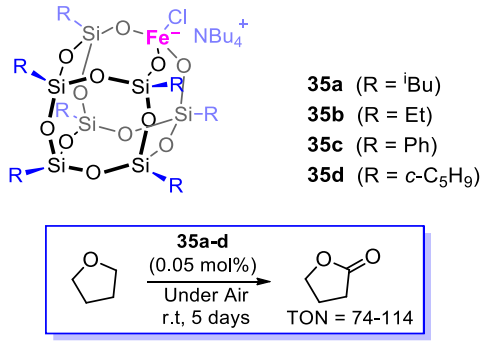

Scheme 13 Fe-POSS complexes for THF oxidation.

More recently, pyrolysis of POSS-based hybrid porous polymers (HPP), led to nitrogen-doped hierarchically porous carbons (N-HPC) used as metal-free catalyst in the oxidative coupling of amines to imines.[72] As depicted in **Scheme 14**, octaphenyl- POSS **36** was reacted with 2,4,6-trichloro-1,3,5-triazine **37** *via* Friedel-Crafts reaction to give **38**. Then, the carbonization of POSS-based polymers **38**, followed by silica etching, led to **39** with enhanced micro- and mesoporosity. N-HPC **39** was tested in the oxidation of a series of benzylamines using oxygen (1 bar) as the primary oxidant, under neat conditions, at 100 °C for 24 h. Furthermore, the recyclability of catalyst **39** was verified for three reuses in the oxidation of 4-methylbenzylamine giving a 97% conversion and selectivity >99%.

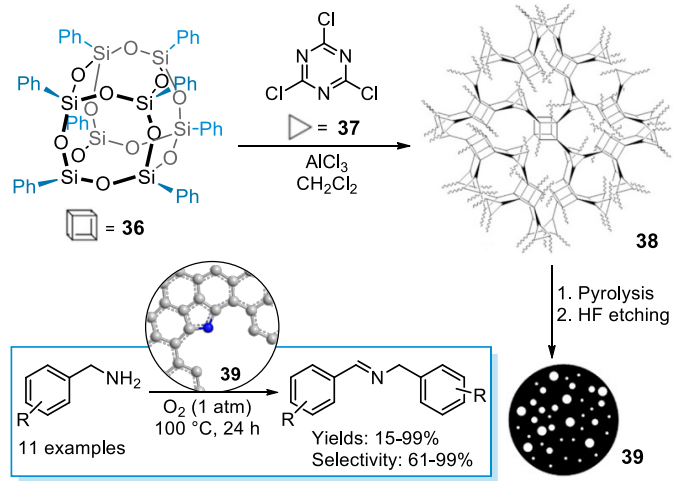

Scheme 14 POSS-based nitrogen doped hierarchically porous carbon oxidation catalyst **39**. Adapted from Ref. 72. Copyright 2017, Wiley-VCH Verlag GmbH & Co. KGaA, Weinheim.

C–C bond formation

Pd catalyzed C–C cross-coupling reactions

The first example dealing with palladium supported POSS nanostructures for C–C couplings was reported by Chang *et al.* in 2010.[73] Amorphous palladium nanoclusters were encapsulated by thiol-functional POSS nanostructures **40** to be used in the Heck reaction between iodobenzene and methyl acrylate (**Scheme 15**). Such catalytic system was prepared starting from the ligand exchange of acetate groups on $Pd(OAc)_2$ with **40**. The thermal treatment of the resulting POSS-Pd(II) complexes led to thiol stabilized Pd(0) nanoclusters **41**.

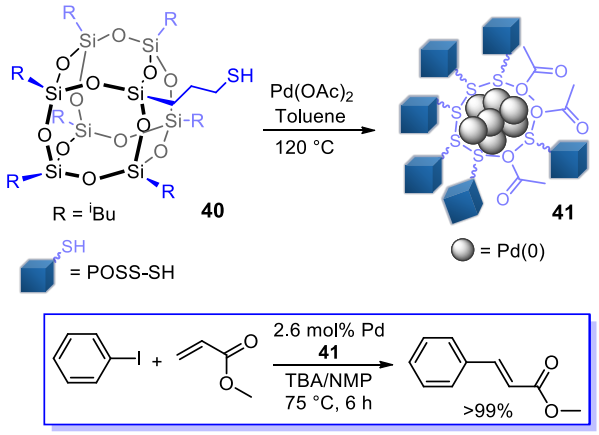

Scheme 15 Pd nanocluster-POSS **41** for Heck reaction.

The coupling of iodobenzene with methyl acrylate was chosen as probe reaction to evaluate the catalytic performance of **41** tested at 2.6 mol% Pd in *N*-methylpyrrolidone (NMP), using tributylamine (TBA) at 75 °C for 6 h. Under these reaction conditions, methyl *trans*-cinnamate was produced in 100% selectivity with a conversion of 99.7%. POSS-Pd nanoclusters **41** were purified by precipitating in MeOH. However, the recycling yields of Pd nanoclusters were about 50 wt % in each cycle.

In 2015 Nischang *et al.* developed monolithic, highly porous, large surface area capillary flow reactors containing POSS nanocages for Suzuki reactions.[74] Hybrid materials based on POSS-Pd(II) complexes were realized by post functionalization of vinyl-POSS, followed by Pd(II) complexation. The resulting capillary flow reactors were tested in Suzuki couplings of seven types of aryl iodides with boronic acids using triethylamine as base, operating with 75/25 acetonitrile/water (%, v/v), fluid contact time of 32.6 min, at 80 °C. Under these reaction conditions, the corresponding biphenyl derivatives were obtained in a broad yield range of 10-90%. In the same year, two novel organopalladium POSS complexes were proposed by Sangtrirutnugul *et al.* for Suzuki-Miyaura reactions.[75] Catalysts **42** and **43** were prepared by reaction between $Pd(COD)Cl_2$ (COD = 1,5-cyclooctadiene) and the corresponding octameric and decameric silsesquioxanes cages, functionalized with pyridine-triazole ligands (**Fig. 9**). Hybrid **42**, featuring one Pd(II) was used as homogeneous catalysts in Suzuki-Miyaura reactions. On the other hand, decameric POSS **43** was employed as heterogeneous catalyst with higher Pd loading (1.61 mmol g^{-1}).

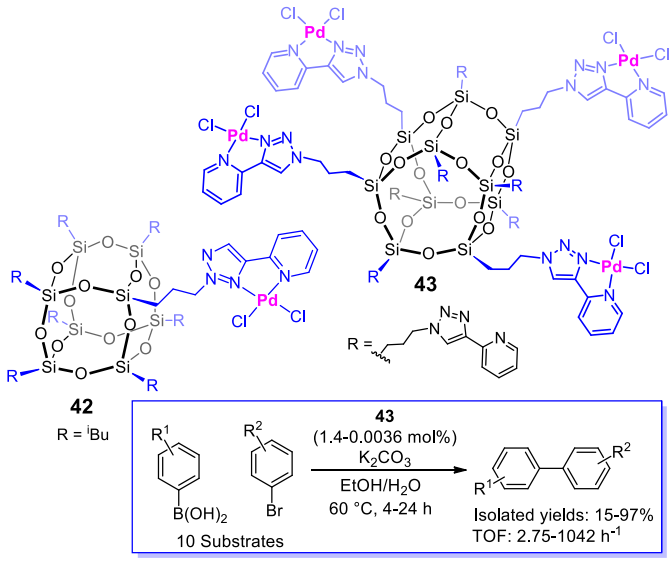

Fig. 9 POSS hybrids **42**-**43** based on pyridine-triazole Pd(II) complexes for Suzuki-Miyaura reactions.

Under the same reaction conditions, catalyst **42** showed slightly higher activity than the heterogeneous catalyst **43** as evidenced by TOF value calculated after 2 h (870 *vs* 690 h^{-1}) in the coupling between phenylboronic acid and 4-bromoanisole. In the above coupling catalysts **43** exhibited good recyclability for five consecutive runs. In order to evaluate the versatility of **43** several aryl bromides and arylboronic acids were tested using K_2CO_3 as base, in an EtOH/H_2O mixture as solvent at 60 °C.

In 2016, hybrid cross-linked networks were prepared by the combination of octa(3-aminopropyl) POSS **19** with terephthalic aldehyde (TPA).[76] This type of material was used as solid support for Pd(II) species in order to obtain a heterogeneous catalyst for Suzuki-Miyaura reactions. Such catalyst was tested at 0.36 mol% with several aryl halides and arylboronic acids, in a mixture EtOH/H_2O, using Na_2CO_3 as base, at room temperature. The biphenyl products were obtained with good to high yields (82-99%) corresponding to TOF values in the 59-550 h^{-1} range.

The influence of POSS nanocages on the catalytic performance for C–C couplings was the subject of a study on a homogeneous pre-catalyst based on POSS nanocages bearing imidazolium tetrachloropalladate moieties (hybrid **44**, **Fig. 10**).[77] The authors made comparison between the POSS-based catalyst **44** and the corresponding POSS-free catalyst (1-butyl-3-methylimidazolium tetrachloropalladate) highlighting the role of the POSS nanocages to reach higher yields in the Suzuki–Miyaura reaction. This result was ascribed to a proximity effect of the imidazolium moieties linked to the nanocaged structure. The same year, Ervithayasuporn *et al.* reported another example of POSS nanostructures functionalized with imidazolium salts **45** as homogeneous catalytic platform for Pd(II) species.[78] The proposed hybrid was used as pre-catalyst at 0.8 mol% for Suzuki-Miyaura reactions with a broad range of conversion (<5-99%) depending on the nature of the selected substrates. The catalytic tests were carried out at 50 °C in a mixture EtOH/H_2O using K_2CO_3 as base for a reaction time in the range of 2-15 h. Under these reaction conditions, the same authors tested Pd(II) pre-catalytic sites supported on imidazolium modified POSS units **46**.[79] This last material was employed as heterogeneous pre-catalyst at 1 mol% for Suzuki-Miyaura couplings between several aryl bromides and phenylboronic acid leading to good conversions (71-100%) and recyclability up to five times.

Very recently, imidazolium functionalized POSS nanocages were successfully grafted onto mesostructured SBA-15 allowing a suitable stabilizing support for Pd (II) pre-catalytic species (**Scheme 16**).[80] The catalytic activity of **47** was investigated toward Suzuki and Heck cross-coupling reactions. In both processes, the catalytic performances were extensively evaluated in terms of turnover frequency, versatility and recyclability. The versatility of **47** was examined with several aryl halides at 0.07 mol% of Pd providing high conversions into the corresponding products. Additional tests were performed by using catalyst **47** with a palladium loading down to 0.0007 mol% showing the outstanding TOF value of 1,721,170 h^{-1} in the Suzuki reaction between 4-bromobenzaldehyde and phenylboronic acid. Catalyst **47** proved to be highly recyclable up to seven cycles without any decrease in the catalytic activity. The recyclability of the material was checked at 0.07 mol% of Pd for six consecutive runs. Interestingly, the catalyst recovered from the sixth cycle was reused for further recycling experiments with decreased amounts of Pd namely for Suzuki (0.007 and 0.0007 mol%) and Heck (0.007 mol%) reactions. The direct comparison of the abovementioned catalytic tests with the analogous ones performed at 0.007 and 0.0007 mol% of Pd with the as-synthesized material assessed the high recyclability of the material.

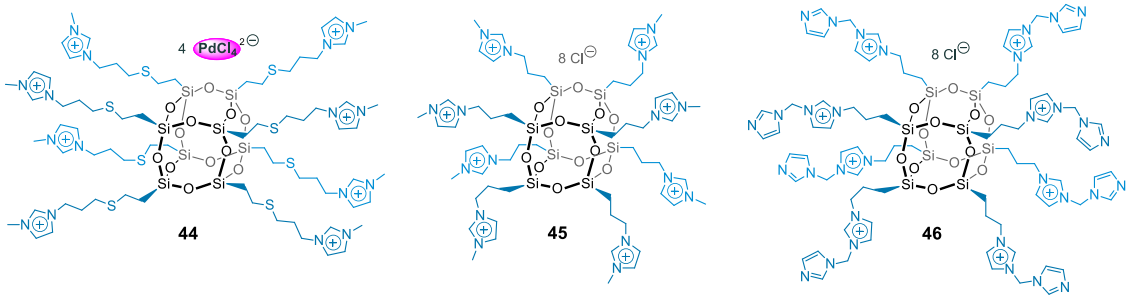

Fig. 10 Imidazolium modified POSS hybrids **44**-**46** as catalytic supports for Pd (II) species.

The presence of the POSS nanocage and the textural properties of SBA, allowed obtaining a uniformly distribution of Pd species within the pore walls, acting as a nanoreactor helping to overcome palladium aggregation and limiting leaching phenomena.

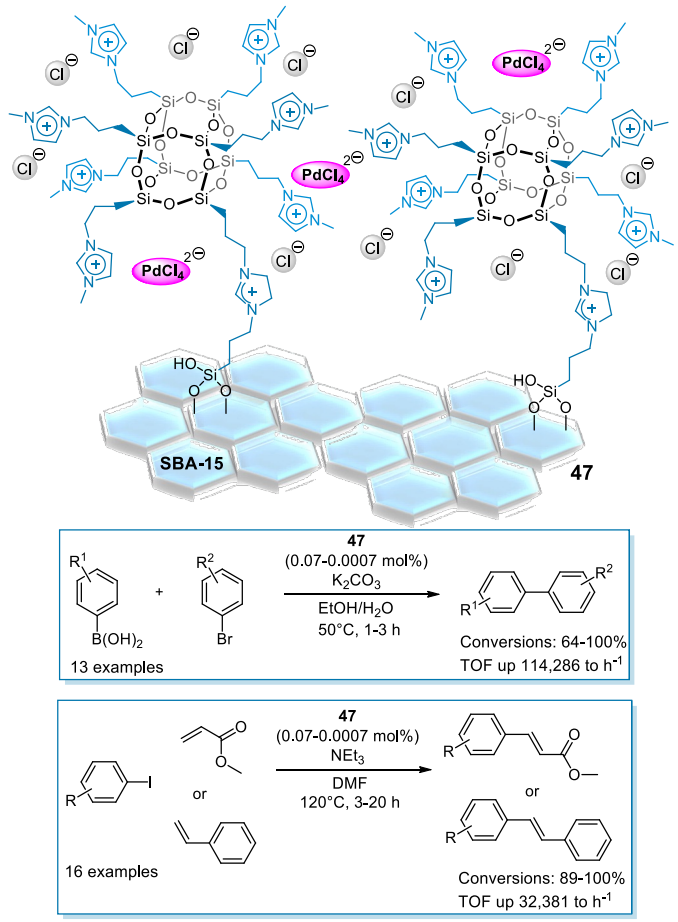

Scheme 16 Pd(II) imidazolium functionalized POSS hybrid **47** for Suzuki-Miyaura and Heck reactions.

In addition to previously mentioned catalysts for C–C cross couplings, Sadjadi and co-workers reported a novel magnetic hybrid of cyclodextrin nanosponges and POSS as stabilizing support palladium nanoparticles.[81] This nanocomposite was employed for Sonogashira and Heck reactions at 2.5-3.0 mol% of Pd. Sonogashira reactions were carried out as copper-free coupling between acetylene and several aryl halides in the presence of K_2CO_3, in water at 90 °C. Heck reactions were performed in ethanol by using several substrates and K_2CO_3. In both catalytic processes the coupling products were obtained with good isolated yields (70-92%) in reaction times in the range of 1.5-5 h.

Michael Addition

In 2015 POSS nanostructures functionalized with diarylprolinol silyl ether were used as organocatalyst for asymmetric Michael addition reactions of aldehydes and arylnitroalkenes.[82] As illustrated in **Scheme 17**, catalyst **50** was synthesized by reaction of 3-azidopropylheptaphenyl POSS **48** with pyrrolidine moiety **49** in dry tetrahydrofuran at room temperature. The obtained POSS supported Jørgensen-Hayashi catalyst **50** was tested with a variety of aldehydes and arylnitroalkenes in dichloromethane at 10 °C giving the corresponding product in high yields (80-90%), enantioselectivities (>96%), and good diastereoselectivities (82:18 to 98:2 $dr_{syn/anti}$). Recycling tests were carried out with prior recovery of **50** from the reaction mixture through precipitation. According to data, catalyst **50** was reused eight times with a slight decrease of activity in terms of yield (from 78% to 70% yield) and ee (from 99% to 97%). Catalyst **50** was employed in a further study concerning the asymmetric synthesis of pyrrolidine **53** starting from the Michael addition of aldehyde **51** to trans-nitroalkene **52**, and subsequent Zn-promoted reductive cyclization process (**Scheme 17**).[83] The use of catalyst **50** did not allowed to epimerization of α-substituted γ-nitroaldehydes.

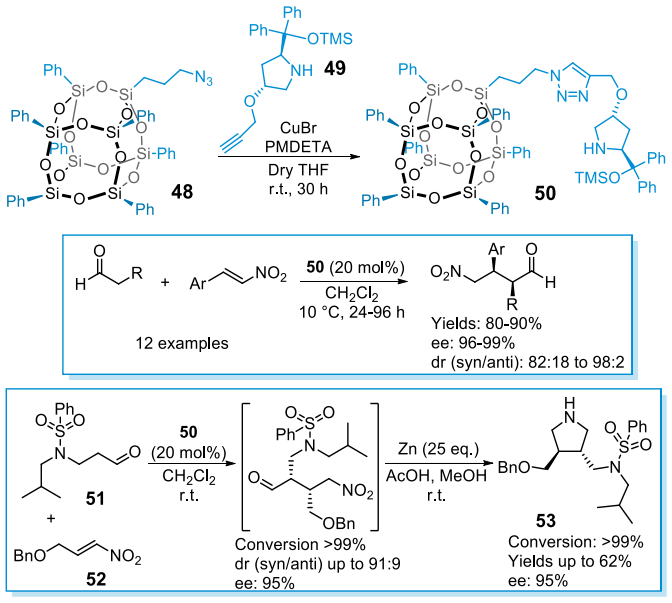

Scheme 17 POSS supported Jørgensen-Hayashi catalyst **50** for Michael additions.

In 2018 chiral pyrrolidine polyhedral oligomeric silsesquioxanes **54** was described by Ervithayasuporn *et al.* as heterogeneous catalyst in the Michael addition of cyclohexanone into nitrostyrenes (**Scheme 18**).[84] The synthetic route of **54** involved the nucleophilic substitution between octabenzylchloride

functionalized POSS and *tert*-butyl (*S*)-2-((1*H*-imidazol-1-yl) methyl) pyrrolidine-1-carboxylate followed by subsequent deprotection. The so obtained material **54** was tested at 0.57 mol% at room temperature with electron-rich and electron-poor nitrostyrenes, giving the corresponding products in high yields (85-91%), diastereoselectivities ($dr_{syn/anti}$ 97:3-99:1), and enantioselectivities (ee 95-98%). The reported yields and selectivities were similar to those exhibited by the homogeneous catalysis[85] and silica gel supported catalyst[86], suggesting that the silsesquioxane core did not interfere with the active chiral pyrrolidine ring. The recyclability of **54** was also verified for four catalytic runs confirming its robustness together with its easy removal from the reaction mixture by simple filtration.

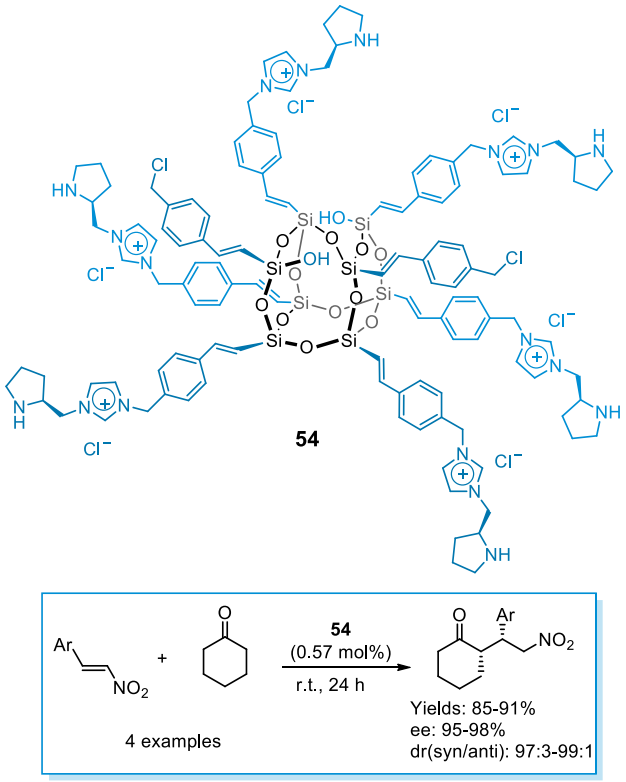

Scheme 18 Chiral pyrrolidine POSS open cage **54** for Michael additions.

Knoevenagel and Henry reactions

POSS monomers were selected by Corma *et al.* as building blocks for the synthesis of hybrid mesoporous materials decorated with amino groups able to catalyze C–C bond formations through Knoevenagel condensation and Henry reactions.[87] These hybrids were prepared based on the structural combination of (octakis(tetramethylammonium)silsesquioxanes and 1,4-bis(triethoxysilyl)benzene. The synthesis was carried out by an acidic self-assembly micellar route in the presence of surfactants as structure-directing agents. Then, the post-synthetic amination treatment of the obtained materials allowed the incorporation of amino groups as basic active sites. The Knoevenagel condensation was catalyzed with a nitrogen loading in the range 2.1-3.4 mol% by reacting benzaldehyde with different substrates such as malononitrile at 30 °C, ethyl cyanoacetate at 60 °C, and ethyl acetoacetate at 80 °C. High yields of 99% were achieved for benzylidene malononitrile and ethyl cinnamate after reaction times of 10 and 3.5 h, respectively, with close to 100% selectivity in both cases. When a substrate with a higher pKa value was used, such as ethyl acetoacetate, the yield of ethyl-2-benzylideneacetoacetate was 66 % after 24 h. The Henry reaction between benzaldehyde and nitromethane was performed at 100 °C with catalyst loading of 3.7 mol% affording nitrostyrene with 99% of selectivity.

In 2015, amine-containing POSS units **55** were grafted onto magnetic nanoparticles in order to be used as heterogeneous catalyst for the synthesis of pyran derivatives through Knoevenagel-Michael tandem reactions (**Scheme 19**).[88] Preliminary catalytic tests were run at room temperature in ethanol by reacting 5,5-dimethylcyclohexane-1,3-dione and malononitrile with an array of isatins. Then, 4-hydroxy-coumarin and barbituric acids were used as different substrates for the condensation with malononitrile and isatins. The corresponding 2-amino- pyrano-3-carbonitrile derivatives were obtained in 69-90% yields. Moreover, catalyst **56** showed good recyclability in the reaction of isatin, malononitrile and dimedone with no considerable decrease in yield (88-84%) for eight consecutive runs.

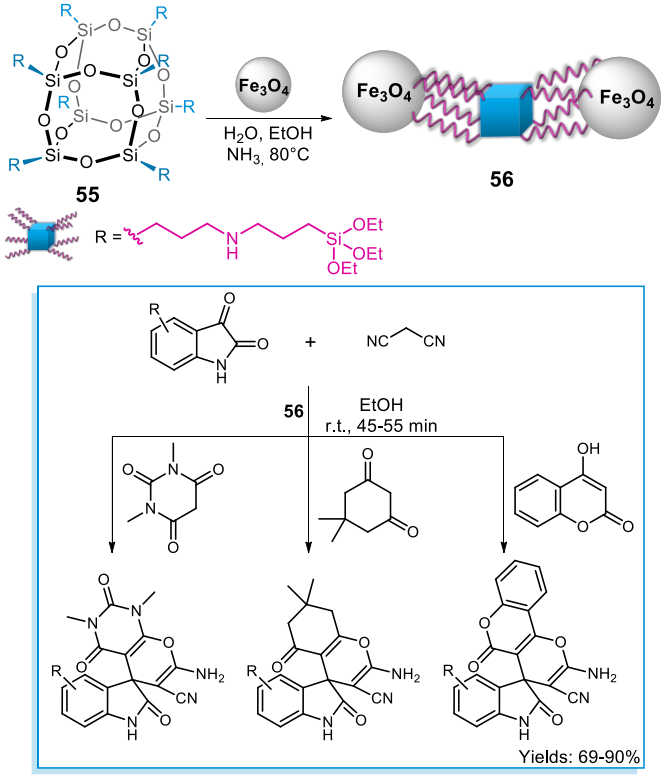

Scheme 19 POSS-based catalyst **56** for the synthesis of pyran derivatives.

In a further work, POSS nanostructures **55** were anchored onto magnetic nanoparticles in the presence of a certain amount of tetraethylorthosilicate (TEOS) to give a core-shell nanocomposite (Fe_3O_4 as the core and SiO_2/POSS as the shell).[89] This nanomaterial was used as catalyst for the synthesis of 1,3-thiazolidin-4-one derivatives by the one-pot condensation of

aldehydes, thioglycolic acid and aniline at 60 °C for 24-36 min without using any solvent. Under optimized reaction conditions, the corresponding product were obtained in high yields (91-94%).

Aldol reactions

In 2015, POSS supported C_2-symmetric bisprolinamide **57a-b** were developed by Ren and coworkers in order to be used as recyclable chiral catalyst for asymmetric aldol reactions between aldehydes and ketones (**Scheme 20**).[90] In the reaction between 4-nitrobenzaldehyde and acetone, **57a** showed higher enantioselectivity than **57b** (ee 95.6% *vs* 82.8%). Then, **57a** was tested with other substrates at room temperature for 20 h, using $Sn(OTf)_2$ as additive, in a mixture DMF/H_2O (9:1). The corresponding adducts were obtained in moderate yields and with high ee (87-96%). POSS-supported catalyst **57a** was recovered *via* simple filtration and reused in five successive runs with slight loss of activity. By comparison with the corresponding unsupported catalyst, POSS hybrid **57a** lowered the yields to some extent, giving higher ee values for acyclic ketone substrates than the non-supported catalyst. Meanwhile, comparable ee values were obtained for cyclic ketones. This behavior was related to steric hindrance arising from the bulky nanocaged structures of POSS units.

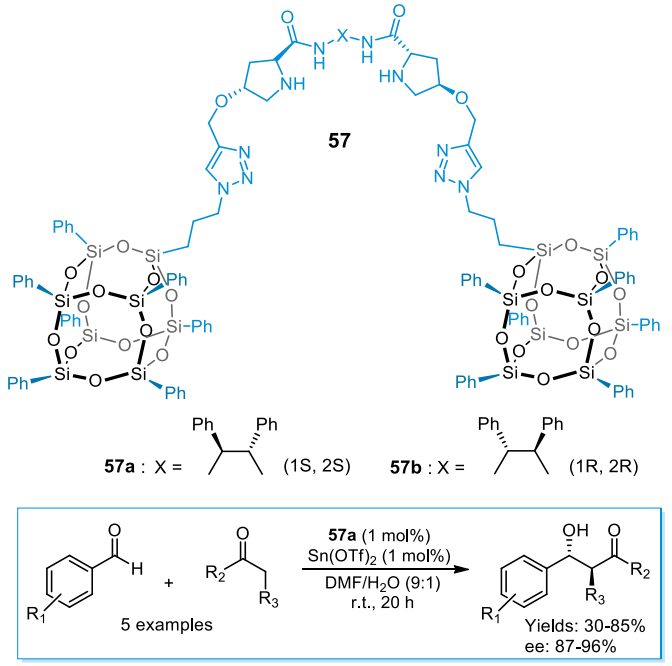

Scheme 20 POSS supported C_2-symmetric bisprolinamide for aldol reactions.

Hydroformylation reactions

In the early 2000s, POSS hybrids started to be used as catalytic systems for hydroformylation reactions. In this field, several studies have been carried out by Hamilton and coworkers. Their interest has been focused on dendrimers based on cubic POSS cores functionalized with phosphine end groups as ligands for metal centers (**Scheme 21**). The synthesis of dendrimers with terminal PR_2 groups (R = Me, Et, Hex, Cy, Ph) was performed by following two strategies: *i)* the radical addition of secondary phosphines to vinyl groups on the periphery of the dendrimer, or *ii)* the reaction of Si–Cl bonds on the dendrimer periphery with lithiated methyl phosphines.[91] The catalytic performance of these hybrids as ligands for rhodium active sites was firstly evaluated by using dendrimer bound phosphines with 24 or 72 arms. The ligand ability of POSS based dendrimers in the hydroformylation of alkenes was confirmed by the formation of the corresponding aldehydes or alcohols depending on the nature of phosphine end groups. In this first study the linear:branched (l:b) product ratio was around 2.4. Improved selectivity was obtained in the hydroformylation of 1-octene with ligand **59**, a POSS-based dendrimer bearing sixteen PPh_2 groups on the periphery.[92] The catalyst was prepared *in situ* from POSS dendrimer and $[Rh(acac)(CO)_2]$ leading to l:b ratios up to 14 and 86% of nonanal. Such catalyst gave much higher linear selectivity than their small molecule analogues (l:b in the range 3-4:1). This behavior was ascribed to a positive dendrimer effect allowing to a favorable bidentate coordination to the metal center.[93]

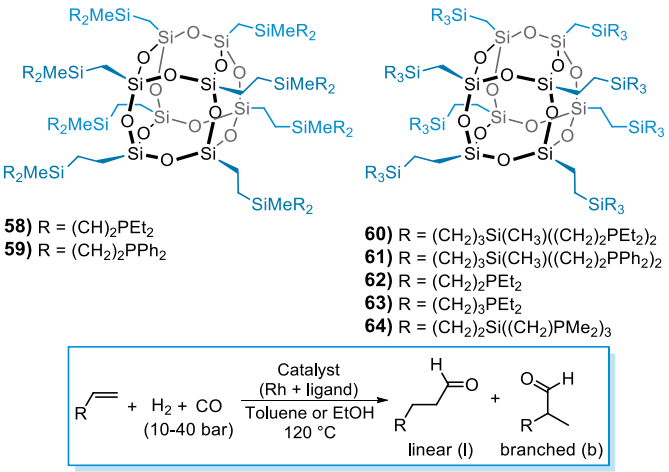

Scheme 21 POSS-based phosphines ligands **58**-**64** for the hydroformylation of alkenes.

The same authors reported 1st and 2nd generation dendrimers based on POSS cores prepared by a divergent synthetic strategy (**58**-**64**). The 1st generation dendrimer was built on either 16 and 24 vinyl or allyl arms formed by successive hydrosilation and vinylation or allylation of vinyl-functionalized POSS. Successive hydrosilation/allylation followed by hydrosilation/vinylation and addition of phosphine produced the 2nd generation dendrimer.[94] The dendrimers were employed as ligands for $[Rh(acac)(CO)_2]$ to be used in the hydroformylation of 1-octene. The alkylphosphine-dendrimers ligands **58** and **60** led to the production of alcohols (1-nonanol and 2-methyloctanol), whereas the diphenylphosphine counterparts **59** and **61** afforded the formation of aldehydes (nonanal and 2-methyloctanal). Linear to branched ratio of 3:1 was recorded for the diethylphosphine compounds while ratios of 12:1 to 14:1 were collected by the diphenylphosphine dendritic molecules. In further studies, first generation **62**-**63** and second generation **60** and **64** alkylphosphine POSS dendrimers were applied as ligands to rhodium for the hydrocarbonylation of linear alkenes (1-hexene, 1-octene, 1-

nonene, prop-1-en-2-ol) leading to alcohols as the main products.[95] The reactions were found to occur *via* the formation of the corresponding aldehydes and subsequent hydrogenation to the alcohols. In some examples slightly higher l:b ratios in the alcohol products were achieved with the dendritic phosphines (3.1:1) than with free triethylphosphine (2.4:1).

The poor activity of the monodentate SemiEsphos phosphine **65** as ligand for rhodium sites was improved by using POSS dendrimers **66** as SemiEsphos supports (**Scheme 22**). In the hydroformylation of vinyl acetate, hybrid ligand **66** combined with $Rh(acac)(CO)_2$ displayed improved performance compared to **65**.[96] The utilization of **66** led to a 60.2% conversion of vinyl acetate and linear to branched ratio of the corresponding aldehyde of 0.086. In the case of ligand **65**, a conversion of 12.9% and a l:b of 2.5 were achieved. These data were collected after 20 h of reaction which was carried out at 80 °C, 40 bar of syngas and P/Rh of 6. The obtained results suggested that two monodentate SemiEsphos molecules giving low activity could be confined in **66** by the molecular architecture of POSS dendrimers to become bidentate and at least partially emulate the more active ESPHOS ligands.

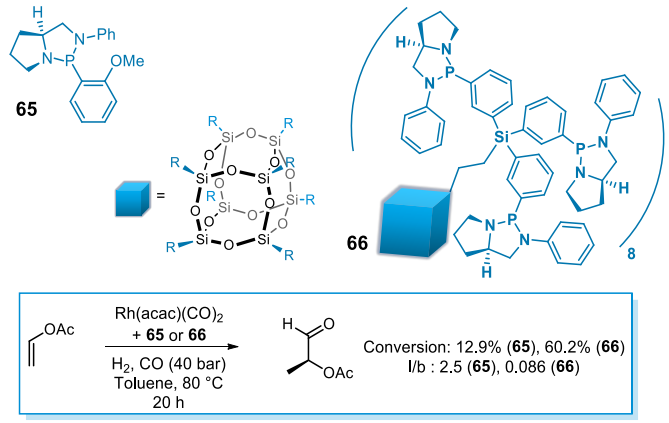

Scheme 22 Esphos ligands **65** and **66** for the hydroformlation of vinyl acetate.

Vogt and coworkers reported the synthesis of POSS-based monodentate phosphite **67** as well as bidentate phosphite **68** as ligands for rhodium catalyzed hydroformylation of 1-octene (**Scheme 23**).[97] The catalytic tests were performed by using $Rh(acac)(CO)_2$ as metal precursor, 20 bar of syngas (CO/H_2 1/1), catalyst preformation time of 1 h, and a reaction temperature of 80 °C. The rhodium complex of POSS monophosphite **67** showed high activity in the 1-octene hydroformylation with an initial turnover frequency of 6800 h^{-1} for a ligand to metal ratio of 10. Such catalytic activity was higher than that provided by catalysts based on electron-withdrawing monophosphites such as the ligand $P(OCH_2CF_3)_3$. However, the regioselectivity of rhodium complex **67** was still low, as expected for a monodentate ligand, with an l:b ratio of around 2.2. Furthermore, the rhodium complex of the bidentate ligand **68** displayed a significantly lower activity owing to the high steric crowding around the metal center, leading to an unselective catalyst with low activity.

In 2010 Vogt *et al.* introduced POSS as versatile unit for molecular weight enlargement of rhodium-based

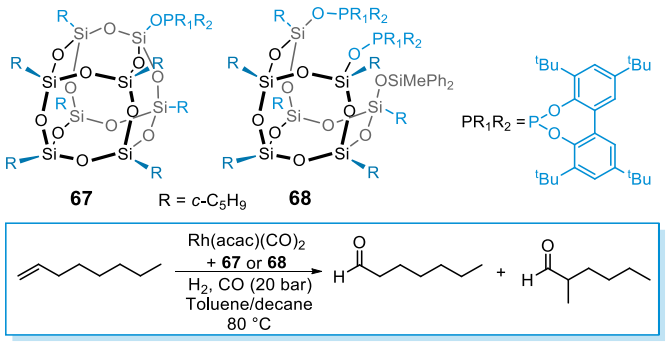

Scheme 23 POSS ligands **67** and **68** for rhodium catalyzed hydroformylation of 1-octene.

homogeneous catalyst.[98] POSS modified triphenylphosphine **70** was prepared as illustrated in **Scheme 24**. Its use as ligand in the rhodium catalyzed hydroformylation of 1-octene was carried out in a continuous flow nanofiltration reactor setup. In a preliminary investigation, the rhodium complex of **70** was tested in an autoclave (batch) experiment in order to be compared with the analogous complex with PPh_3 as ligand. The turnover frequencies were calculated at 20% conversion to be 1350 h^{-1} and 3150 h^{-1} for POSS enlarged PPh_3 and unmodified PPh_3, respectively. The rhodium complex of **70** gave a 99% conversion after 17 h, when used in a continuous flow membrane reactor at 20 bar of syngas and 80 °C. The 1-octene conversion remained greater than 90% for almost two weeks. Over this period, the adopted catalytic system displayed the same regioselectivity for unsupported PPh_3 with l:b ratio of 2.5. The combined use of $Rh(acac)(CO)_2$ as catalytic precursor and **70** as ligand highlighted a breakthrough in the sustainable conversion of alkenes under homogeneous conditions without the usual drawback of tedious and often expensive catalyst recovery and recycling.

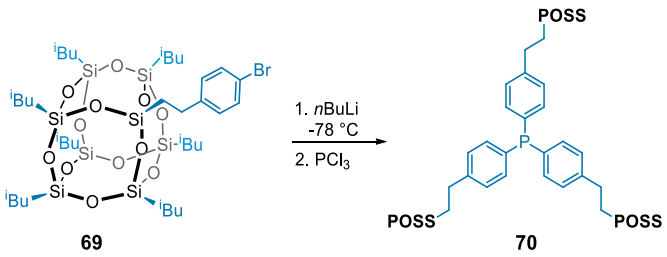

Scheme 24 POSS ligands **70** for rhodium catalyzed hydroformylation.

Metathesis reactions

The first use of silsesquioxanes as precursors for catalysts able to promote olefin metathesis dates back to 1994.[99] Feher *et al.* reported molybdenum silsesquioxanes **71** complex as efficient homogeneous catalyst reaching 150 turnovers within 20 s after mixing 4800 equivalents of 1-octene to catalytic amounts of the Mo-silsesquioxane. The metathesis reaction of 1-octene to 7-tetradecene was complete purging ethene from the system. Similar results were achieved for 1- and 2-pentenes as well as cis-2-octene. In 2006, Moore and coworkers prepared the pentacoordinated molybdenum complex **72** bearing completely condensed POSS nanocages.[100] This complex was synthesized

by reaction of $(c\text{-}C_5H_9)_7Si_8O_{12}(OH)$ with trisamidomolybdenum(VI) propylidyne. The homogeneous hybrid **72** was able to selectively catalyze alkyne metathesis over alkyne polymerization showing high activity at room temperature. The catalytic behavior of this Mo-POSS complex resulted analogous to that of its silica supported counterpart.

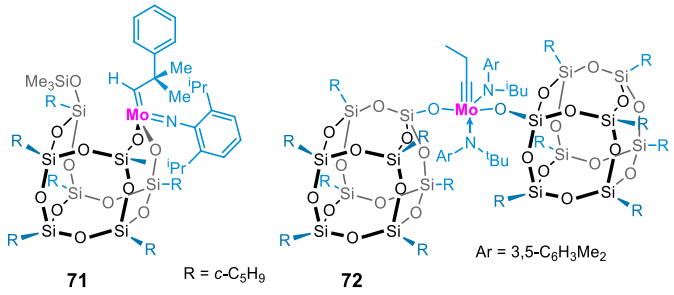

Fig.11 Mo-POSS catalysts **71**-**72** for metathesis reactions.

In 2013, Grela *et al.* reported POSS-tagged Grubbs-Hoveyda complexes **73** and **74** as olefin metathesis nanocatalysts (**Fig. 12**).[101] The ring-closing metathesis (RCM) reaction of diethyl diallylmalonate was selected to study the activity of the synthesized complexes. Both **73** and **74** proved to be almost as active as the parent Hoveyda complexes achieving quantitative conversions at 1 mol% and room temperature. Complex **73** displayed slightly higher activity than its unsaturated analogue **74**. Then, a broad scope of substrates was chosen to further evaluate the catalytic performance of POSS tagged catalyst **73**. Metathesis reaction were performed at 1 mol% of **73** in dichloromethane or toluene as solvent and reaction temperature in the range 25-80 °C. Under this reaction conditions, the metathesis products were obtained in 52-99% yields. Batchwise and continuous organic solvent nanofiltration was adopted to separate the catalyst from the post-reaction mixture. Some commercial membranes were tested in batch mode being Starmem 228 the more efficient showing stable separation performance with a catalyst rejection of approximately 100%, product rejection in the range of 10%, and Ru concentration in the permeate was below 3 ppm. In continuously stirred tank reactor mode after 2.5 h a conversion of around 84% was achieved being both catalyst recycling and catalyst stability still a challenge.

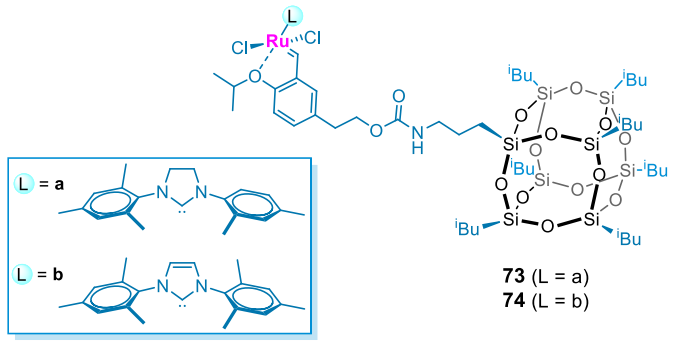

Fig. 12 Ru-POSS complexes **73**-**74** for metathesis reactions.

More recently, POSS-modified ruthenium complexes **75**-**78** were synthesized and applied as nanocatalysts in ring closing metathesis reactions (**Fig. 13**).[102] Firstly, in order to evaluate the activity of **75**-**77** diethyl diallylmalonate was chosen as probe substrate to react at 25 °C in toluene by using a catalytic loading of 0.5 mol%. From these preliminary investigations catalyst **75** was the most active with turnover frequency of 14.8 min^{-1} at 20% conversion (TOF of 6.2 $min^{-1}$and 9.2 min^{-1} for **76** and **77**, respectively). A further molecular weight enlargement of ruthenium complexes was performed with the synthesis of catalyst **78**. The ring closing metathesis of diethyl diallylmalonate was carried out using both **75** and **78** with a ruthenium loading of 0.05 mol%. After 2 h, conversions of 91% for **78** and 85% for **75** were afforded. When both catalysts were tested at 0.2 mol %, the authors reported TOF values at 20% conversion of 24.0 min^{-1} for **75** and 26.0 min^{-1} for **78**. Recycling experiments of **75**, **78** and the Grubbs–Hoveyda second generation catalyst were performed with a ceramic membrane in a cat-in-a-cup setup. The Grubbs-Hoveyda second generation catalyst was employed as benchmark and, although showing a higher initial conversion, a conversion decrease faster than **75** and **78** was observed with an overall conversion of 41% over 4 cycles (total TON = 825). Catalyst **75** having one POSS-unit led to an overall conversion of 49% (total TON = 980). Catalyst **78**, containing a POSS-unit on the NHC ligand as well as on the benzylidene unit, still exhibited a conversion of nearly 50% in the fourth cycle. The overall conversion with catalyst **78** reached 69% corresponding to a total TON of 1380. Such results evidenced the importance to enlarge both the NHC- and the benzylidene moiety of metathesis catalysts, so that catalyst decomposition is not driven forward by the removal of stabilizing components during filtration. The post reaction solutions were analyzed in order to estimate the Ru content. Leached ruthenium from **78** was below 1 ppm in all 4 runs. On the other hand, with catalyst **75** Ru leaching was significantly higher in the first two cycles, whereas the highest leaching was observed for POSS-free Grubbs-Hoveyda second generation catalyst.

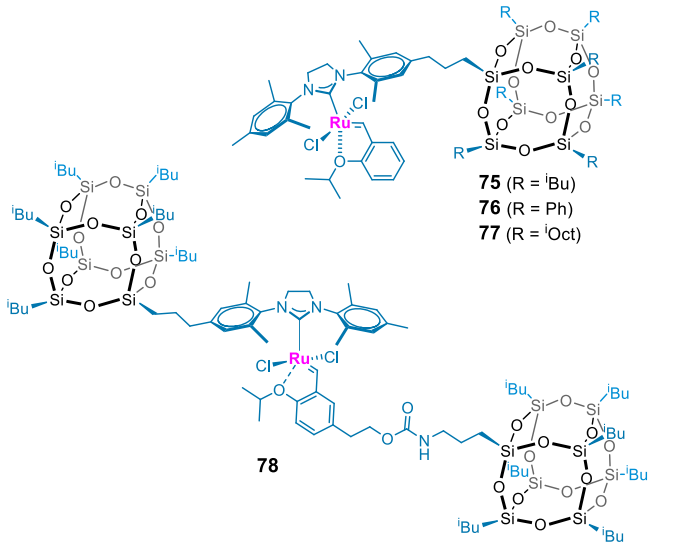

Fig. 13 Ru-POSS complexes **75**-**78** for metathesis reactions.

CO_2 conversion into cyclic carbonates

Carbon dioxide conversion embodies the concept of moving toward more sustainable catalytic processes. The synthesis of cyclic carbonates from CO_2 and epoxides is a key example to produce valuable chemicals from a valorized industrial waste. In this context, a plethora of both homogeneous and heterogeneous catalytic systems has been reported in the literature.[103, 104] In the last few years, POSS nanocages have been selected as catalytic platforms for the conversion of CO_2 into cyclic carbonates. The good outcoming of the catalytic process is influenced by many parameters including the nature of the nucleophilic active species, the use of co-catalysts, the temperature, the CO_2 pressure, the reaction time, etc.

Herein, for the sake of clarity, we report POSS based catalytic systems together with their turnover frequency values (TOF) strictly calculated considering the amount the nucleophilic active sites (X^- = Cl^-, Br^-, I^-).[105] The first example dealing with the conversion of carbon dioxide catalyzed by POSS based hybrids has been reported in 2015.[106] Imidazolium modified POSS molecules **79** (**Fig. 14**) have been prepared and tested as homogeneous nanocatalyst for the production of cyclic carbonates showing improved activity compared to the unsupported 1-butyl-3-methylimidazolium salt. This behavior was ascribed to a proximity effect related to the higher local concentration of imidazolium active sites surrounding the inorganic silsesquioxanes core. Imidazolium functionalized POSS molecules were tested with styrene oxide, epichlorohydrin and 1-butene oxide under optimized reaction conditions using (isopropanol as co-solvent, 150 °C, 4 MPa of CO_2) showing turnover frequency (TOF) values in the 138.7-706 h^{-1} range. Two years later, Koo *et al.*[107] used POSS molecules **80** and **81** as building blocks (**Fig. 14**) for the preparation of heterogeneous catalysts *via* the free-radical polymerization of their organic moieties, namely vinyl or allyl groups to afford cross-linked networks. The obtained materials were tested with several epoxides at 110 °C and 0.76 MPa of CO_2 pressure. According to collected data, the ionic POSS scaffold **80** endowed with imidazolium chloride active sites displayed slightly better catalytic performance (TOF up to 35.7 h^{-1}) by comparison with the analogous hybrid bearing trialkyl ammonium chloride moieties (TOF up to 27.7 h^{-1}).

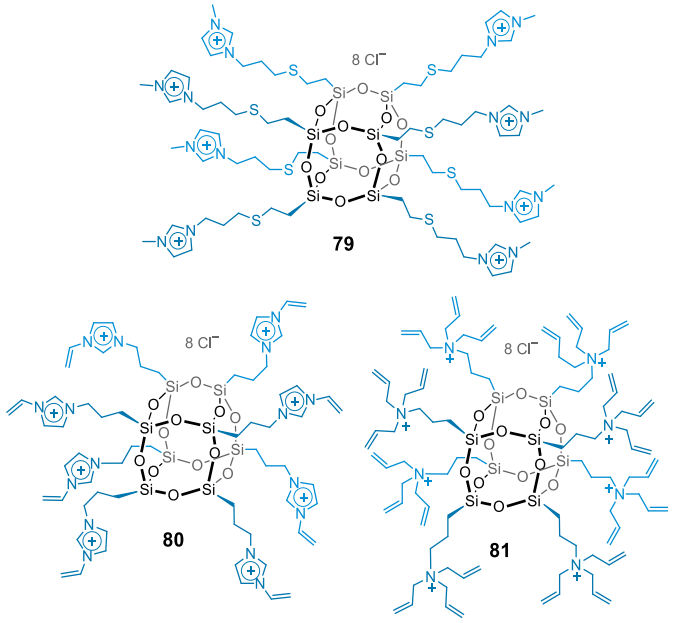

Fig. 14 POSS molecular structures **79**-**81** for CO_2 conversion.

Recently, Liang and co-workers[108] prepared a series of hybrid porous polymers made up of carbazole units acting as organic linkers between POSS nanocages. The combined use of these materials with tetrabutylammonium bromide (TBAB) has been proposed for the conversion of CO_2. The catalytic tests were performed at 120 °C and 2 MPa of CO_2 pressure using TBAB at 0.5 mol%. The authors selected styrene oxide as starting substrate to study the influence of carbazole moieties. TBAB alone gave a conversion of styrene carbonate of 32%, whereas POSS-carbazole polymers used as the sole catalysts did not show any catalytic activity. The synergistic activity of nucleophilic bromide species, carbazole N–H sites, and silanol groups was proven when POSS-carbazole polymers were used in the presence of TBAB giving higher conversions up to 85%. Even if POSS-carbazole polymers were recovered from the reaction mixture to be recycled, TBAB was not reused, thus limiting the recyclability of the whole catalytic system.

In 2019, highly performing metal-free heterogeneous catalysts **84** based on POSS nanostructures functionalized with imidazolium salts have been developed. As showed in **Scheme 25**, a broad series of catalytic materials was prepared by using a modular synthesis to obtain imidazolium modified POSS nanocages grafted onto amorphous silica (SiO_2) and mesostructured SBA-15.[109] The synthetic procedures were designed to study the influence of the solid support (SiO_2 *vs* SBA-15) and the effect of both nucleophilic species (Cl^-, Br^-, I^-) and imidazolium alkyl side chain length. All the solids were tested as heterogeneous organocatalysts for the conversion of epoxides and CO_2 into cyclic carbonates in solvent-free reaction conditions. The effect of the nucleophilic species led to the overall order of activity I^- > Br^- > Cl^-. The main goal of this research was to maintain the high catalytic activity of unsupported imidazolium modified POSS,[106] due to the proximity effect of the imidazolium units linked to the POSS nanocage, with the benefits of heterogeneous catalysis, in

terms of recyclability, without the need of other co-catalytic species with Brønsted or Lewis acid functionalities. The proposed materials were easily recyclable as well as highly active toward the formation of cyclic carbonates affording very high turnover numbers (TON) and productivity values up to 7875 and 740, respectively.

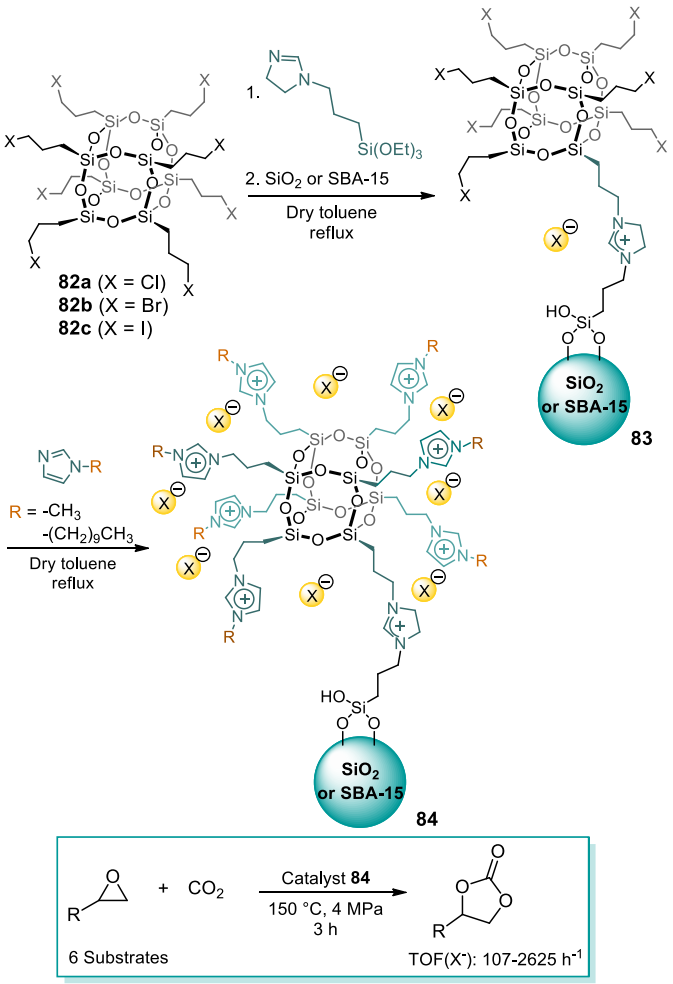

Scheme 25 Silica-supported imidazolium-modified POSS **84** used for the synthesis of cyclic carbonates from CO_2 and epoxides.

In the same year, two novel hybrid materials based on highly crosslinked imidazolium networks were prepared from POSS molecular building blocks **82b-c** in order to be used as heterogeneous catalysts bearing different nucleophilic species (bromide and iodide).[110] The solids were synthesized by using the simple one-pot procedure depicted in **Scheme 26**. The solids **85** and **86** were tested as the sole catalyst under metal- and solvent-free reaction conditions showing full selectivity toward the formation of cyclic carbonates. High TON and productivity values up to 5502 and 1081, respectively for glycidol at 100 °C and up to 4942 and 1122 for epichlorohydrin at 150 °C after 3 h, were afforded. Such outstanding productivity values were ascribed to the optimal organic/inorganic (*i.e.* imidazolium moiety/POSS support) weight ratio. The good recyclability of the materials (up to four cycles) allowed considering them as promising candidates for continuous flow technologies.

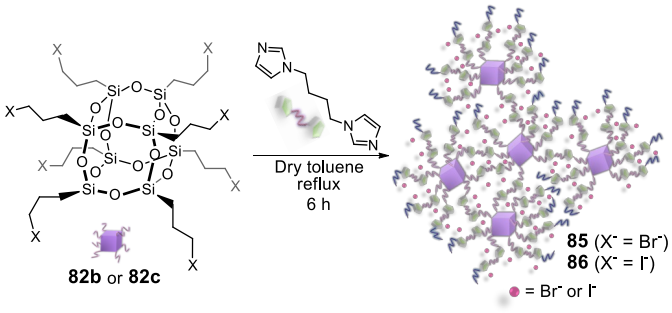

Scheme 26 Synthesis of imidazolium cross-linked POSS nanohybrids.

Since 2018[111] Chen *et al*. reported some studies on hybrid materials from POSS nanostructures for the synthesis of cyclic carbonates. POSS and viologen-linked porous cationic frameworks **87a** and **87b** were prepared by Zincke reaction between octa(aminophenyl)silsesquioxane and two viologen linkers (**Fig. 15**). The obtained materials **87a** and **87b** showed high surface area (174 and 383 m^2g^{-1}), high amount of viologen sites (6.56 and 5.72 mmol g^{-1}) and enriched Si–OH groups. Both hybrids were tested as heterogeneous catalyst in the absence of any solvent and co-catalytic species. The conversion of epichlorohydrin into the corresponding carbonate was chosen to compare the activity of the solids under different reaction conditions in terms of temperature (80-100 °C), CO_2 pressure (1-0.1 MPa) and time (6-72 h). High cyclic carbonate yields were achieved (84-99%) being the solid **87b** slightly more active then and **87a** according to the better nucleophilicity of Br^- than Cl^- active species. Material **87b** retained its activity for five consecutive cycles and catalyzed the conversion of several epoxides with TOF values in the range 0.44-5.77 h^{-1}. In 2019, the same research group reported another series of silanol enriched viologen-based ionic porous polymers from octavinyl-POSS **26**.[112] These materials were prepared by the Heck reaction between **26** and two selected viologen ionic linkers (**Fig. 15**, **88a** and **88b**). The obtained hybrids polymers possessed tunable surface areas (150-562 m^2g^{-1}), pore volumes (0.41-1.82 cm^3g^{-1}) and ionic sites (0.92-1.47 mmol g^{-1}). As showed in **Fig. 15**, **88a** and **88b** were used as heterogeneous catalysts for the fixation of carbon dioxide into epoxides under mild conditions (30-80 °C, CO_2 pressure of 0.1 MPa). In particular **88a** was tested at 7.25 mol% with several epoxides with TOF values in the range 0.28-0.44 h^{-1}. In the reaction between CO_2 and epichlorohydrin catalyst **88a** proved to be more active than a benzene-based viologen ionic monomer similar to viologen ionic active sites in the porous polymer. The authors ascribed this behavior to the presence of Si–OH groups within **88a** playing a synergistic catalytic role together with Br^- active species. Furthermore, the recyclability of **88a** was easily assessed for five consecutive runs using epichlorohydrin as starting epoxide.

Very recently, Chen and co-workers reported a further series of ionic porous hybrid polymers with POSS derived silanols bearing imidazolium bromide moieties (**Fig. 15**, **89a**, **89b**).[113] The synthetic procedure consisted, also in this case, in a solvothermal Heck reaction between octavinyl-POSS **26** and two selected organic ionic linkers. The resulting materials possessed high surface areas up to 464 m^2g^{-1}, large pore volumes up to

1.65 cm^3g^{-1}, highly dispersed ionic sites, and *in situ* formed Si–OH groups. The presence of silanol groups came from the cleavage of Si–C and Si–O bonds during the synthesis of the imidazolium based cross-linked networks. The catalytic activity of both **89a** and **89b** was investigated in the conversion of epichlorohydrin into the corresponding cyclic carbonate in the absence of any solvent, co-catalyst or other metal additives under atmospheric CO_2 pressure and different temperatures (25-80 °C). **89b** was reused for five cycles and its versatility was assessed at 1.37 mol% with several substrates.

It is worth noting the influence of the organic linkers on the catalytic performance of the above mentioned ionic porous hybrid polymers. In the CO_2 fixation into epichlorohydrin (80 °C, 48 h, 0.1 MPa CO_2 pressure), imidazolium based hybrid polymers exhibited **89a** and **89b** better catalytic activity (TOF 1.32-1.45 h^{-1}) by comparison with the previously introduced viologen based cross-linked polymers[112] (TOF 0.28-0.26 h^{-1}). The catalytic performances of **89a** and **89b** (96-98% yields) slightly improved when compared to those of the homogeneous ionic linkers (93-94%) under the same reaction conditions. In this context, the heterogeneous catalytic performance was described as a synergistic combination of highly dispersed nucleophilic active sites (Br^-) and hydrogen bond donor Si–OH groups. According to the proposed reaction mechanism, the presence of silanol groups leads to the C–O polarization of the epoxide. Then, the nucleophilic species attacks the activated epoxide leading to the ring-opening of the epoxide to form an intermediate stabilized by hydrogen bond donor Si–OH groups. The insertion of CO_2 allows to an
alkyl carbonate intermedia te generating the cyclic carbonate by intramolecular ring-closure.

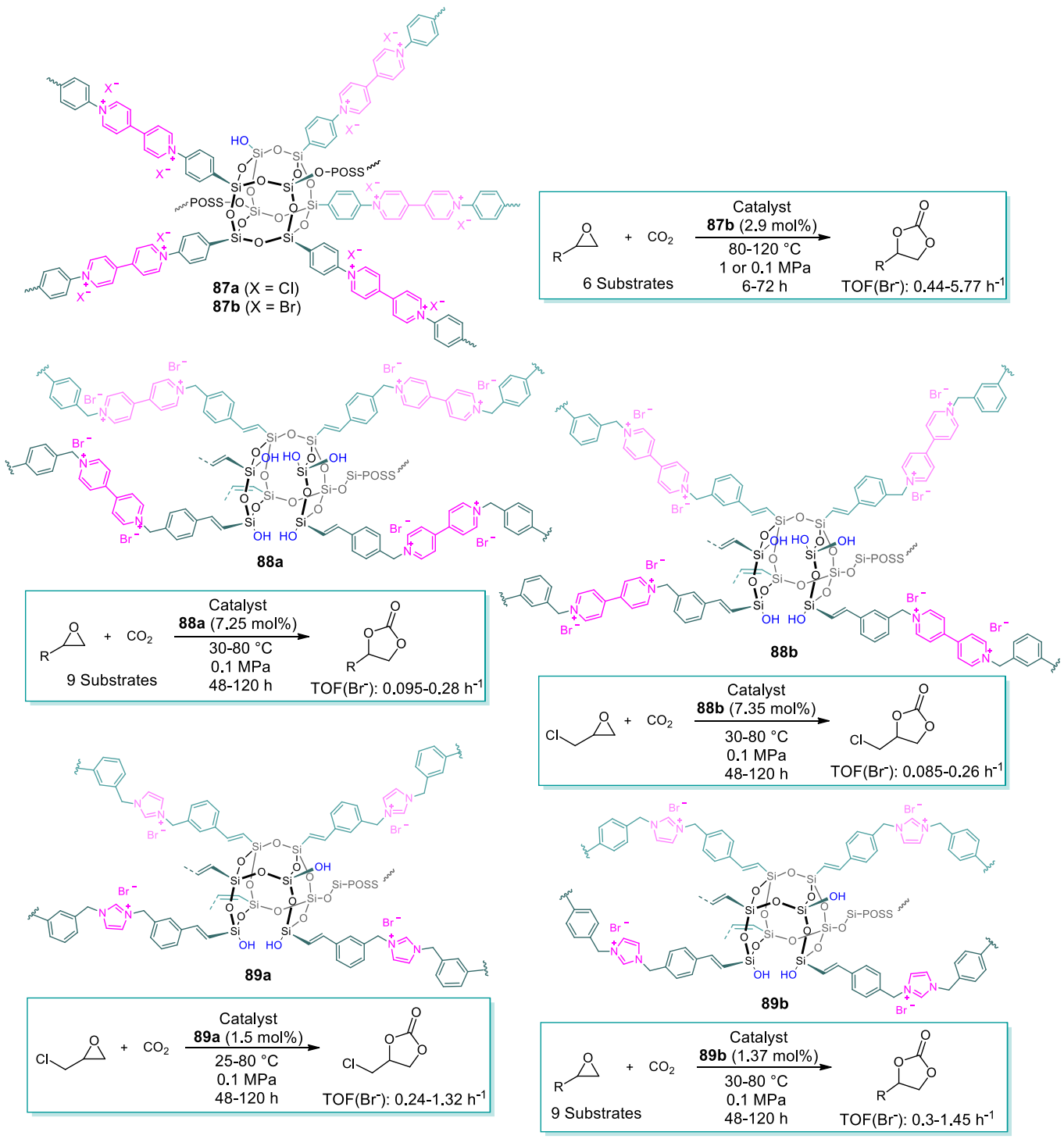

Fig. 15 Ionic porous hybrid polymers **87**-**89** with POSS-derived silanols for the conversion of CO_2 into cyclic carbonates.

Esterification and acetylation reactions

In 2016, POSS-based porous ionic polymer **91** was developed as heterogeneous acid catalyst for the esterification of oleic acid with alcohols (**Scheme 27**).[114] Catalyst **91** was synthesized starting from the copolymerization of octavinyl-POSS **26** and 1-vinyl-3-propane sulfonate imidazolium **90**. Then, the obtained solid was treated with H_2SO_4 to give the final material. Catalyst **91** was tested at 2 mol% in the esterification of oleic acid with methanol, at 70 °C for 3 h. The corresponding oleate was produced with 94% conversion and >99% selectivity. The catalytic activity of **91** was at least comparable to that of the homogeneous H_2SO_4 (98% conversion). On the other hand, the analogous non porous POSS-free polymer gave a lower

conversion of 79.2%. This result proved that the presence of POSS units in the polymer matrix played an essential role for the formation of porous networks ensuring a better catalytic performance. Moreover, recyclability of **91** was assessed for four consecutive runs with a slight decrease in the catalytic activity.

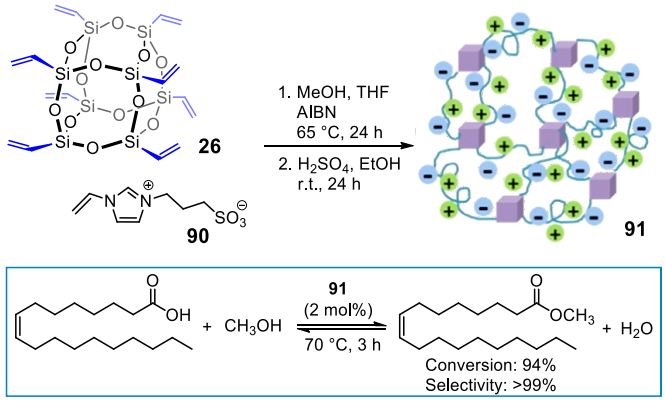

Scheme 27 POSS based ionic polymer **91** for the synthesis of oleate. Adapted from Ref. 114. Copyright 2016, Elsevier B.V.

In a further study, POSS-derived solid acid catalysts were synthesized through free radical copolymerization of octavinyl-POSS **26** with sodium *p*-styrene sulfonate **92** (**Scheme 28**).[115] The obtained materials **93** showed tunable surface areas, and high hydrophobicity. Catalysts **93** exhibited high activity and selectivity toward glycerol derivatives, which were even higher than that of homogeneous H_2SO_4. The proposed catalytic process were the esterification of glycerol with acetic acid and the acetalization of glycerol with benzaldehyde. The esterification of glycerol with acetic acid was carried out in toluene, at 120 °C for 2 h, with a catalytic loading of 0.003 mol%. On the other hand, the acetalization of glycerol with benzaldehyde was performed at 30 °C for 2 h, by using a catalytic loading of 0.0017 mol%. In both processes, catalyst **93** was reused up to five consecutive cycles without showing any significant decrease in the catalytic activity. The promising performance of these heterogeneous acid catalysts was mostly ascribed to the combination of their hydrophobicity, wettability for various organic substrates, and high surface areas.

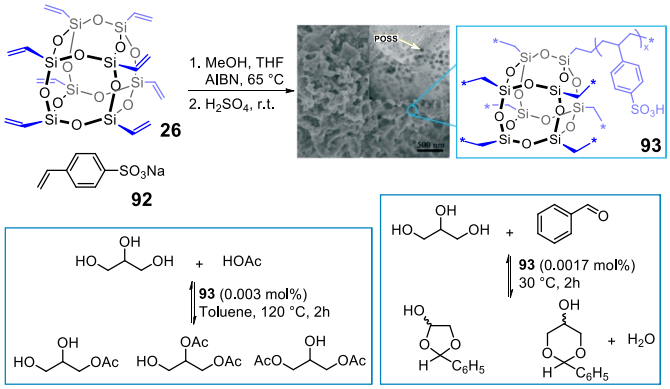

Scheme 28 POSS based ionic polymer **93** for glycerol transformations. Adapted from Ref. 115 with permission from The Royal Society of Chemistry.

Reduction reactions

Hydrogenation and hydrosilylation reactions

POSS molecules have been used as stabilizing support for metal nanoparticles able to catalyze hydrogenation reactions. In 2007, Saab *et al.* reported palladium nanoparticles stabilized with POSS units for the direct hydrogenation of 1,4-diphenylbutadiyne.[116] For doing so, octa(3-aminopropyl) POSS units **19** were treated with $Pd(OAc)_2$ in methanol. According to TEM and SEM studies, the obtained material included 2-5 nm diameter Pd crystallites in a POSS layer, which aggregate to form spherical secondary structures of about 50 nm in diameter (**Fig. 16**). The catalytic activity of the POSS-stabilized Pd NPs was observed *via* direct hydrogenation experiments in a microbalance under hydrogen exposure at 1 atm.

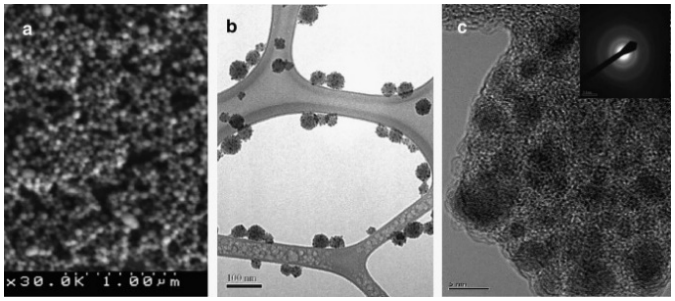

Fig. 16 a) SEM image of POSS-Pd NPs, b) low resolution TEM image, c) HR-TEM image of one NP, in the inset the diffraction rings generated by Pd dots. Reproduced from Ref. 116. Copyright 2007, Elsevier B.V.

Yang and coworkers synthesized octa(diacetic aminophenyl) silsesquioxanes (OAAPS) as stabilizing agents for Pd, Pt and Ru nanoparticles.[117, 118] The metal colloids showed excellent stability owing chelating effect of the cubic POSS to metal nanoparticles. Pt and Pd nanoparticles stabilized by OAAPS were used as catalysts for the hydrogenation of some phenyl aldehydes. Hydrogenation reactions were carried out in a mixture $EtOH/H_2O$ at 30-40 °C under hydrogen atmospheric pressure. Both OAAPS stabilized colloidal catalysts were recovered by switching the pH of the solution to promote their precipitations. Pt and Pd colloids were reused up to five and eight times, respectively, still showing good catalytic performances. However, the catalytic activities of the Pd colloids were not as high as those of the metal nanoparticles stabilized by polyaryl ether dendrons.

Monticelli *et al.* included POSS nanostructures into electrospun polymer nanofibers for the design of two novel catalytic systems one able to promote the degradation of sulforhodamine B,[119] the other able to promote the hydrogenation of stilbene.[120] In the latter case, Pd nanoparticles immobilized on the surface of poly(L-lactic acid) PLLA nanofibers containing aminopropylisobutyl POSS uniformly dispersed into the polymer matrix (**94**, **Scheme 29**).[120] In this study, amino modified POSS were chosen as polymer additive able to interact with the metallic precursor, likely through a coordinative mechanism. Conversely to the PLLA polymer matrix, which does not show any tendency to retain the metal precursor, the dispersion of POSS-NH_2 in the PLLA nanofibers promoted the formation of metal nanoparticles on the fiber

surface. TEM measurements evidenced a uniform distribution of Pd NPs, with an average size of ca. 4 nm, along the fibers. This hybrid material was successfully used as heterogeneous catalyst (at 1.7 mol%) for the hydrogenation of stilbene in methanol as solvent, under H_2 atmosphere (1 atm). After 3 h of reaction, a quantitative conversion of stilbene into diphenylethane was detected by ^{1}H NMR analysis as well as the complete absence of peaks belonging to PLLA/POSS-NH_2. Furthermore, XPS analysis of the hydrogenated product after separation from the nanofibers proved the support capacity of retaining the catalyst during the hydrogenation reaction.

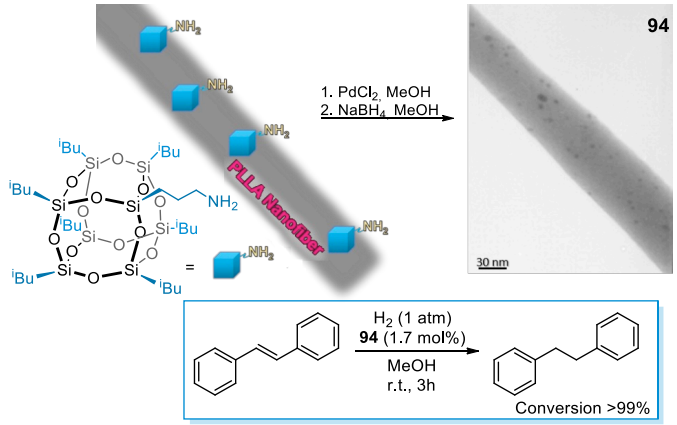

Scheme 29 Pd NPs on PLLA/POSS-NH_2 **94** for the hydrogenation of stilbene. Adapted from Ref. 120. Copyright 2013, American Chemical Society.

In 2012, Li and coworkers reported the synthesis of **95** and its use as heterogeneous chiral catalyst for asymmetric transfer hydrogenation of aromatic ketones in aqueous medium (**Scheme 30**).[121] It is worth to point out that in **95** POSS nanocages bring quaternary ammonium salts with phase transfer function and organorhodium sites as chiral Cp*RhTsDPEN catalyst [(Cp* = pentamethyl cyclopentadiene and TsDPEN = 4-(methylphenylsulfonyl)-1,2-diphenylethylenediamine)]. From the above, the catalytic tests were performed without using Bu_4NBr as additive. The asymmetric transfer hydrogenation of aromatic ketones was carried out at 0.4 mol% Rh loading, with HCOONa, at 40 °C for 1 h. Under these reaction conditions, catalyst **95** afforded high conversions (84-99%), good enantioselectivity (91-96%), and turnover frequency values in the range 209-250 h^{-1}. The catalytic performances were ascribed to the phase transfer action of the quaternary ammonium salt in a two phases reaction system, whereas the good enantioselectivity was related to the unchanged chiral microenvironment. Catalyst **95** was quantitatively recovered *via* nanofiltration to be successfully used for twelve consecutive runs.

Porous styryl-linked POSS polymers were used as platinum supports generating a suitable heterogeneous catalyst for the hydrosilylation of styrene with dimethylphenylsilane (0.1 mol% of Pt, room temperature, in toluene).[122]

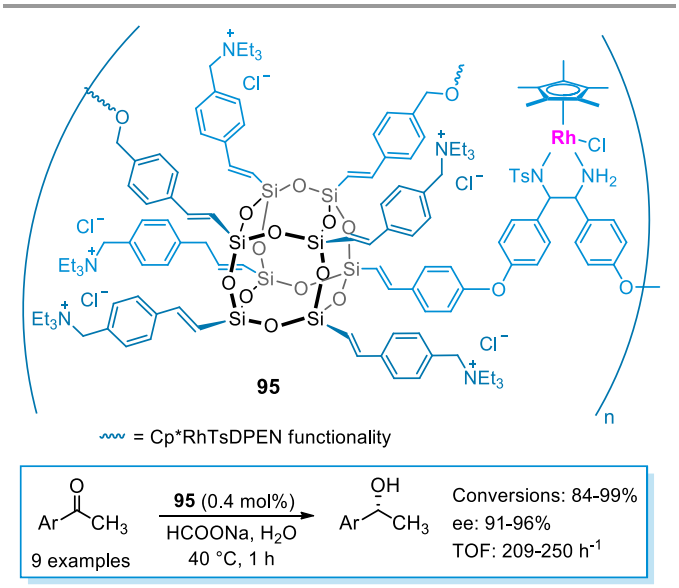

Scheme 30 Rh-POSS catalyst **95** for asymmetric transfer hydrogenation of aromatic ketones.

After 1 h of reaction, the catalyst led to a quantitative conversion into the corresponding product. The authors stated that the catalytic performance of platinum-supported POSS polymers was comparable to that of commercial Karstedt's catalyst, but with the difference that Pt-POSS nanocomposite was more easily separated from the reaction mixture facilitating the recyclability of the catalyst itself.

Reduction of nitrophenol and organic dyes

In the recent literature concerning the catalytic reduction of nitrophenols, POSS nanostructures have been applied as catalytic platforms for gold, silver, and palladium nanoparticles. In 2016, Nischang *et al.* used vinylPOSS polymers as component of hybrid porous monolithic capillary columns decorated with thiol groups for anchoring gold nanoparticles of various sizes (5-100 nm). These materials were used in the *p*-nitrophenol reduction over several catalytic cycles in continuous flow operation using an aqueous fluid phase containing sodium borohydride. Furthermore, their best performance was achieved with gold nanoparticles of 10 nm.[123] The reduction of *p*-nitrophenol was chosen as probe reaction to test the catalytic performances of silver NPs (10-30 nm) immobilized onto cross-linked hydrogels made up from a the polyaddition reaction of EDTA dianhydride with PEG_{600} followed by the addition of octa(3-aminopropyl) POSS as nano-crosslinker.[124] This hybrid hydrogel was employed as heterogeneous catalyst in aqueous media by using $NaBH_4$ as reducing agent allowing the quantitative conversion of *p*-nitrophenol into *p*-aminophenol within 120 s. In 2019, imidazolium functionalized POSS were employed as catalytic support for silver or copper nanoparticles (**96-97**, **Fig. 17**).[125] The hybrid material **96** catalyzed the *p*-nitrophenol reduction into *p*-aminophenol, using $NaBH_4$ as reducing agent, in aqueous medium at room temperature.

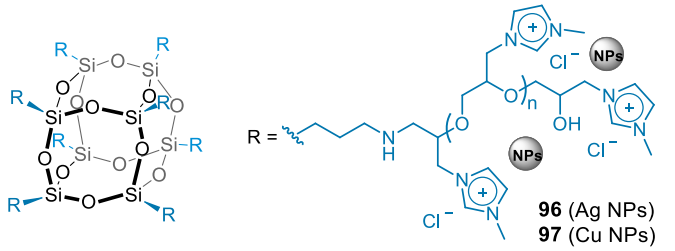

Fig. 17 Imidazolium modified POSS as catalytic support for Ag and Cu NPs.

Kibar *et al.* developed the *in-situ* growth of silver on the surface of POSS-based support particles by using mussel-inspired polydopamine (PDA) coating.[126] The POSS based nanocomposite support were prepared by free radical mechanism in one-step emulsion polymerization of methacryl-POSS monomer (M-POSS). Smooth spherical shape poly(M-POSS) hybrid particles (200-400 nm) were covered by the functional amine and catechol groups of PDA. Silver layer were growth on PDA@poly(M-POSS) nanocomposite template. The catalytic activity of Ag@PDA@poly(M-POSS) nanocomposite **98** was checked by pseudo-first order kinetic reaction of nitrophenol (**Fig. 18**). Compared to similar silica-based catalysis, Ag@PDA@Poly(M-POSS) nanocomposite particles showed better catalytic properties for the degradation of a highly toxic environmental pollutant such as *p*-nitrophenol in the presence of $NaBH_4$.

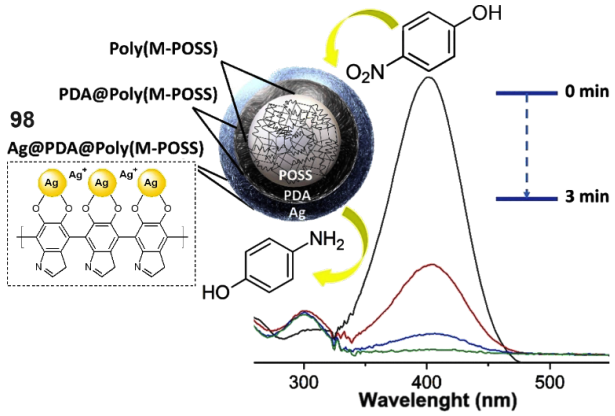

Fig. 18 4-nitrophenol reduction catalyzed by Ag@PDA@Poly(M-POSS) **98**. Reproduced from Ref. 126. Copyright 2019 Elsevier Ltd.

Very recently, POSS units have been modified with ammonium salts in order to be used as platform for palladium nanoparticles (**Fig. 19**).[127] The catalytic performances of nanohybrid **99** were explored in the reduction several substrates including some organic dyes (methylene blue, methyl orange, rhodamine 6G, rhodamine B, congo red) and in the degradation of nitrophenols. Catalyst **99** showed excellent dispersibility and stability in aqueous medium. It was reused four times in degrading methylene blue and three times in reducing *p*-nitrophenol showing a low decrease of the catalytic efficiency. Furthermore, compared to conventional Pd/C catalyst, **99** displayed higher catalytic performance for degrading colored dyes and reducing different nitrophenols in water. These results have been ascribed to the strong coordination of Pd NPs with the quaternary ammonium salt groups of POSS nanocages.

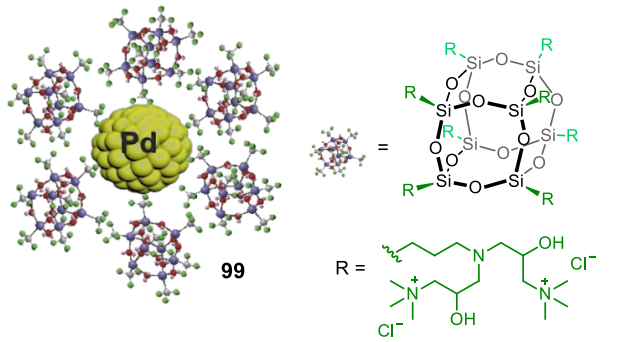

Fig. 19 Pd NPs supported on POSS units **99** bearing alkylammonium salts. Adapted from Ref. 127. Copyright 2019, Elsevier B.V.

Click reactions

In the last few years, POSS nanostructures have been employed as hybrid supports for copper active sites able to promote click reactions in aqueous medium. Catalyst **97** was tested in the reaction between phenyl acetylene, benzyl chloride and sodium azide to synthesize 1-benzyl-4-phenyl-1,2,3-triazole.[125] These substrates were chosen for a preliminary optimization of the reaction conditions. After 12 h at 50 °C, catalyst **97** led to the highest product yield of 82%. Then, additional catalytic tests were performed with several alkynes and substituted benzyl halides. The click reaction of phenyl acetylene allowed higher yields (67-82%) by comparison with aliphatic alkynes (6-22%).
In a further work, azide-alkyne cycloaddition reactions were carried out by using copper(II)-POSS-bridged Schiff bases **100**.[128] As illustrated in **Scheme 31**, catalyst **101** was prepared by reaction of POSS ligands **100** with $Cu(OAc)_2$ as metal precursor, at room temperature for 24 h. Under previously optimized reaction conditions, catalyst **101** was tested at 2.6 mol% in the reaction between a wide scope of substituted phenyl acetylenes and the mixture of benzyl bromides/chlorides and NaN_3 to produce the corresponding 1,4-disubstituted-1,2,3-triazoles with yields in the range of 89-96%.

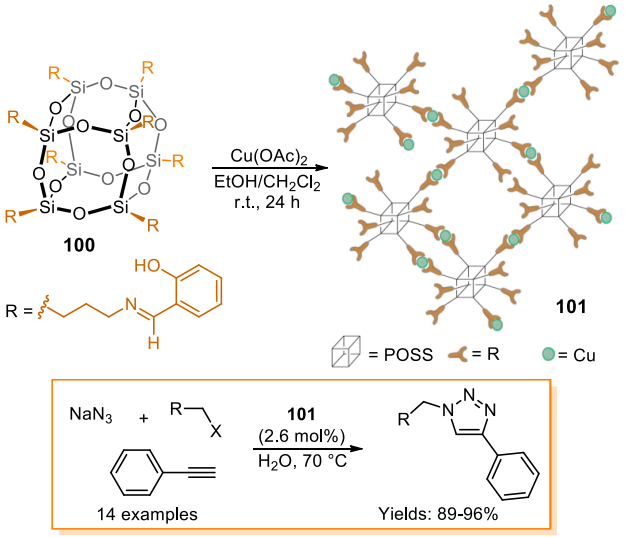

Scheme 31 Cu-POSS hybrid **101** as catalyst for azide-alkyne cycloadditions. Adapted from Ref. 128. Copyright 2015 Elsevier B.V.

Alkene polymerization

Since the 1990s, the catalytic activity of metal silsesquioxanes has been investigated in the olefin polymerization by using transition metal complexes in combination with co-catalytic species such as organoaluminium or organoboron compounds. Incompletely condensed silsesquioxanes have been considered versatile tools and precursors for the design of homogeneous model supports in developing silica supported olefin polymerization catalysts.[129]

In 1991, Feher *et al.* reported the synthesis of vanadate silsesquioxane **102** and its use as catalyst for the polymerization of ethylene upon activation with $AlMe_3$ or $Al(CH_2SiMe_3)_3$ (**Fig. 20**).[130, 131] Catalyst generated from **102** achieved turnover number values in the range of 1000-1500 when the polymerization was carried out at 25 °C and 1 bar of ethylene pressure. The analysis of the polymer gave a number average molar mass (M_n) of 21,000 and weight average molar mass (M_w) of 47,900. Furthermore, the catalytic activity of **102** was tested with other olefins. The polymerization of propene gave rise to an atactic polymer with M_w<10,000, whereas the polymerization of 1,3-butadiene allowed obtaining a product being >95% trans-1,4-polybutadiene. One year later, in order to elucidate the reaction mechanism in the ethylene polymerization, the activation of catalyst **102** was examined in the presence of $Al(CH_2SiMe_3)_3$.[132] The authors, found that the formation of the active catalyst implied alkyl transfers and the coordination of vanadium oxo bond to the Lewis acidic aluminium site. The best catalytic performance was obtained by using two equivalents of AlR_3 agent. Higher amounts of AlR_3 led to the reduction and deactivation of the metal centers, whereas lower amounts were not enough to reach the complete catalyst activation. More recently, a series of vanadium-based silsesquioxanes was synthesized by reacting VCl_4 with incompletely condensed silsesquioxanes having from one to four silanol groups. Once prepared, vanadium containing silsesquioxanes complexes **103-106** were studied as pre-catalysts in olefins polymerization (**Fig. 21**).[133] Ethylene polymerization was performed by using several activating co-catalytic species (Al/V = 1000-10000), under 5 bar of ethylene, at 30 °C for 30 min. Ultra-high molar mass polyethylene (M_w up to $4 \cdot 10^6 g \cdot mol^{-1}$) were achieved with methylaluminoxane (MAO) and $Al(^iBu)_3/[Ph_3C][B(C_6F_5)_4]$ as activators. After activation with $EtAlCl_2$, complexes **103-106** turned out to be highly active in the polymerization of ethylene with increasing productivity in the order **103**<**104**<**105**<**106**. POSS ligand with the highest denticity conferred to bimetallic V-silsesquioxane **106** the best catalytic performance with a productivity of 169.0 $kg_{PE}\ g_V^{-1}$ $(0.5\ h)^{-1}$. The improvement of the catalytic activity with increasing ligand denticity was observed also when Et_2AlCl was used as activator. MAO and borate activators, which were supposed to form the cationic active centres, resulted less effective than common organoaluminium compounds leading to a different order of productivities of the vanadium pre-catalysts (**105**<**103**<**106**). Furthermore, V-complexes **103-106** were tested in the polymerization of 1-octene yielding isotactic-rich polymers with mmmm pentad content up to 75%.

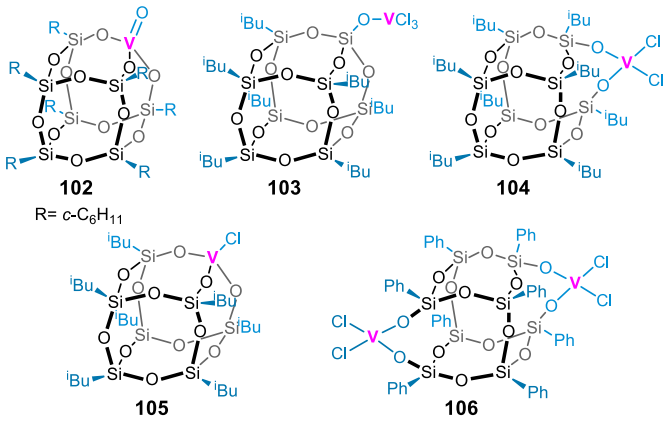

Fig. 20 Vanadium containing POSS nanocages **102**-**106**.

Duchateau and coworkers developed a number of completely condensed metal silsesquioxanes complexes (**Fig. 21**, **107**-**115**). The cuboctameric hydroxysilsesquioxane $(c\text{-}C_5H_9)_7Si_8O_{12}(OH)$, prepared by hydrolysis of $(c\text{-}C_5H_9)_7Si_8O_{12}Cl$, was applied as molecular precursor for the synthesis of fully condensed metal silsesquioxanes and as model support for silica-grafted olefin polymerization catalysts.[134, 135] The silsesquioxane ligands were introduced on group 4 metals (Ti, Zr) by either chloride metathesis or protonolysis. Dichloride (**107a**-**b**) and monochlorides (**109a**-**b**) complexes, activated by MAO, formed active ethylene polymerization catalysts. In the presence of MAO, metal complexes bearing a tridentate silsesquioxane ligand, $[(c\text{-}C_5H_9)_7Si_8O_{12}]$-MCp'' (M = Ti (**110a**), Zr (**110b**)), generated active ethylene polymerization catalysts proving that silsesquioxane and siloxy ligands were easily substituted by MAO. The silsesquioxane and siloxy bis(alkyl) titanium complexes **108a** and **108b**, after activation with $B(C_6F_5)_3$, led to catalysts with ethylene polymerization activity of 18 $Kg_{PE}\ g_{Ti}^{-1}h^{-1}$ retaining the M–O bond unaffected.

Both dimeric zirconium and hafnium benzyl complexes (**111a** and **111b**, respectively) promoted ethylene polymerization even without using co-catalytic species. Their catalytic activity was related to the targeted dimeric structures allowing a synergistic activation between the two metal centers.[136] This activating synergism was improved by using $B(C_6F_5)_3$ as co-catalyst leading to the formation of dimeric mono(benzyl) cations through the removal of one of the two benzyl groups from the dimers **111a** and **111b**. The obtained cationic monobenzyl dimers showed much higher ethene polymerization activity (26 $kg_{PE} \cdot g_{Zr}^{-1} \cdot h^{-1}$ and 27 $kg_{PE} \cdot g_{Hf}^{-1} \cdot h^{-1}$) than that of the neutral dimers **111a** (0.11 $kg_{PE} \cdot g_{Zr}^{-1} \cdot h^{-1}$) and **111b** (0.06 $kg_{PE} \cdot g_{Hf}^{-1} \cdot h^{-1}$). $B(C_6F_5)_3$ activated **111a** (M_w = 6600, M_w/M_n = 2.3) led to a was much lower polyethylene molecular weight than the corresponding hafnium system (Mw = 82000, M_w/M_n = 3.2). The higher activity of the Hf-catalyst generated from **111b** was ascribed to the lower thermal stability of the analogue Zr-complex at higher polymerization temperatures. The reported results were collected by running the catalytic tests at 80°C, under 5 bar of ethylene pressure for 7 min. Interestingly, the corresponding titanium silsesquioxane

compound $[(c\text{-}C_5H_9)_7Si_7O_{12}]TiCH_2Ph$, monomeric in solution, resulted inactive in ethylene polymerization.

Silsesquioxane-bonded zirconocene complexes **112-115** were examined as soluble models for silica-tethered olefin polymerization catalysts.[137, 138] In this work, ethylene polymerization experiments were performed in toluene at 25 °C and 2 bar of ethylene by using the homogenous silsesquioxane-substituted zirconocene dichlorides **112-115** (0.1 mol% of Zr). All Zr-complexes were activated by MAO thus generating active single site ethylene polymerization catalysts. The polymerization activities of **112–115** (up to 42 $kg_{PE}{\cdot}g_{Zr}^{-1}{\cdot}h^{-1}$) resulted lower than those of the corresponding non-silsesquioxane complexes (up to 62 $kg_{PE}{\cdot}g_{Zr}^{-1}{\cdot}h^{-1}$).

Silsesquioxane-borato complexes **116a** and **116b** (**Fig. 21**) were used as molecular model for silica-grafted perfluoroborato cocatalysts in ethylene polymerization with a study focused on the stability of B–O bond in the presence of $Cp_2Zr(CH_2Ph)_2$.[139] Silsesquioxanes-borates resulted unstable toward zirconium alkyl species.

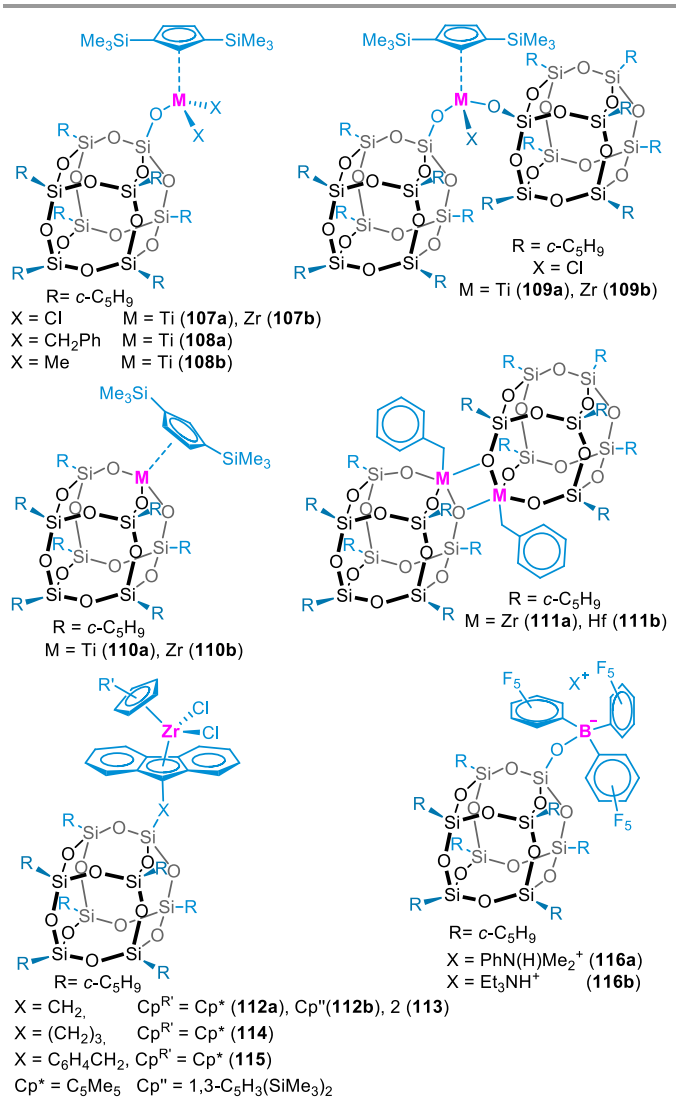

Fig. 21 Metal silsesquioxanes complexes **107-115** and silsesquioxane borate complexes **116a-b** as catalyst model for olefin polymerizations.

Ammonium silsesquioxane borate **116a** gave single site ethylene polymerization catalysts which were tested at room temperature, 5 bar of ethylene pressure in five minutes of reaction time (M_w = 566,000 and M_w/M_n = 2.3). In particular, the reaction of $Cp_2Zr(CH_2Ph)_2$ with **116b** was considerably slower suggesting as first step of reaction the protonolysis of one of the benzyl groups by the ammonium cation, due to the easier protonolysis for $PhN(H)Me_2^+$ than for the less acidic Et_3NH^+. The formed cationic alkyl complex was rapidly transformed into an inactive cationic silsesquioxane complex. The formation of $B(C_6F_5)_3$ explained the fact that ethylene polymerization activity was still observed. Based on these results, the authors concluded that the B–O bond in silica-grafted borates is expected to be labile. Therefore, under influence of transition-metal alkyls, silica-grafted borates were assumed to be transformed into physisorbed borane, which could be considered as the actual cocatalyst.

Since 2011, Tembe and coworkers reported the synthesis and the application of a broad scope of metal silsesquioxanes complexes in the olefins polymerization (**117-125**, **Fig. 22**). Firstly, the authors reported Ti (IV)-POSS complexes **117** and **118** for the polymerization of ethylene at high temperatures in combination with ethylaluminum sesquichloride (EASC) as co-catalyst.[140] Under optimized reaction conditions (100 °C, in toluene, 27.6 bar of ethylene, Al:Ti ratio of 500, 1 h), complex **117** showed higher productivity of (54.9 $Kg_{PE}\ g_{Ti}^{-1}\ h^{-1}$) than **118** (43.3 $Kg_{PE}\ g_{Ti}^{-1}\ h^{-1}$). Under the same reaction conditions, unless for a lower ethylene pressure (20.7 bar), the anchored group (IV) metal complexes **119-125** were evaluated in polymerization of ethylene in combination with EASC.[141, 142] According to data, for complexes **119-122** the achieved productivities were in the range values 2.5-42.1 $Kg_{PE}\ g_{catalyst}^{-1}\ h^{-1}$ with the overall order of activity **119**>**120**>**121**>**122**.

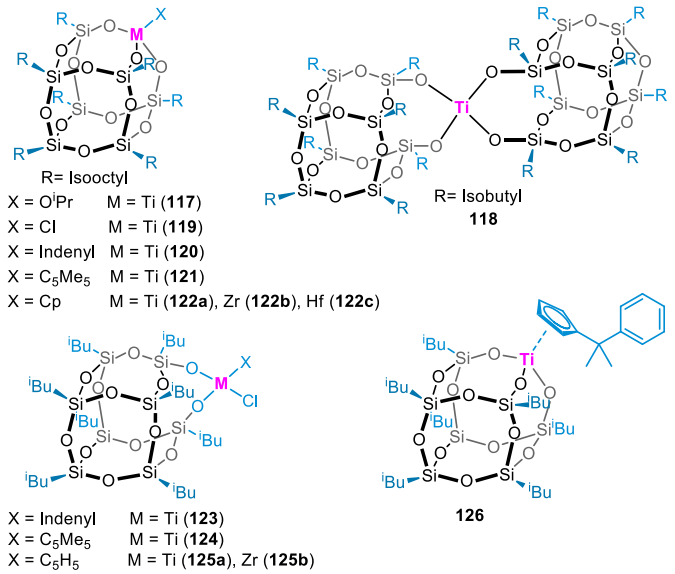

Fig. 22 Metal silsesquioxanes complexes **117-126** as catalyst model for olefin polymerizations.

By changing metal active sites, titanium based complex **122a** exhibited better productivity than zirconium- or hafnium-POSS complexes (**122a**>**122b**>**122c**). On the other hand, complexes

123-**125** displayed worst catalytic activity with productivity values in the range 1.9-28 $Kg_{PE}\ g_{catalyst}^{-1}\ h^{-1}$ (**123**>**124**>**125**). In this case as well, Ti-complex **125a** proved to be more active than the analogous Zr-complex **125b**.

In 2015, titanium complex **126** was employed as silica model for ethylene trimerization. In the presence of MAO (Al/Ti= 1000), at 30 °C, 5 bar of ethylene and reaction time of 30 min Ti-POSS **126** led to a 1-hexene productivity of 6.45 $Kg_{1\text{-hexene}}\ g_{Ti}^{-1}\ h^{-1}$.[143]

Ziegler-Natta type catalysts prepared from the reaction between Mg based silsesquioxanes ligands with $TiCl_4$ (compounds **127** and **128**, **Fig. 23**).[144] Ethylene polymerization was carried out at 90 °C, 34.5 bar of ethylene, in 2-methylpropane as solvent. The bimetallic complexes **127** and **128**, activated by $AlEt_3$ (Al/Ti = 25), led to a polyethylene productivity of 111 $Kg_{PE}\ g_{Ti}^{-1}\ h^{-1}$. This value was higher than that obtained by using the commercial Ti/Mg/SiO_2 silica supported catalyst with the same bimetallic content (60 $Kg_{PE}\ g_{Ti}^{-1}\ h^{-1}$). By using such silsesquioxane based Ziegler-Natta type catalysts, the produced polyethylene showed M_w =140,000 and molecular mass distribution M_w/M_n = 5.5.

More recently, Li *et al.* reported the synthesis of weakly entangled polyethylene by using a POSS modified Ziegler-Natta catalyst (**Fig. 24**).[145] POSS units **129** were employed as ligands able to coordinate multiple $MgCl_2$ molecules serving as electron donors with a cage structure able to further incorporate $TiCl_4$. POSS/$MgCl_2$ adducts were firstly adsorbed and uniformly distributed on the surface of Macro-SiO_2 forming nanoaggregates with a mean size of 48 nm. Then, $TiCl_4$ sites were immobilized on these nanoaggregates serving as horizontal separators for isolating the active $TiCl_4$ and the growing polyethylene chains. A controlled distribution of active sites in the heterogeneous silica supported Ziegler-Natta type catalytic system **130**, illustrated in **Fig. 24**, led to the production of ultra-high molecular weight polyethylene up to $2{\cdot}10^6$ g/mol corresponding to a productivity of 27.2 $Kg_{PE}\ g_{Ti}^{-1}\ h^{-1}$ and a molecular weight distribution (MWD) of 9.5. These results were collected by running the catalytic tests at 60 °C, in toluene as solvent, at 3 bar of ethylene pressure, in the presence of and $AlEt_3$ as cocatalyst (Al/Ti = 100).

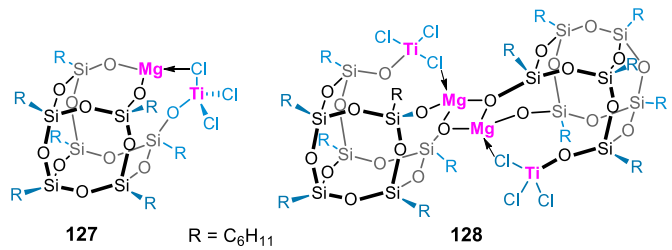

Fig. 23 Silsesquioxane based Ziegler-Natta type catalyst for ethylene polymerization.

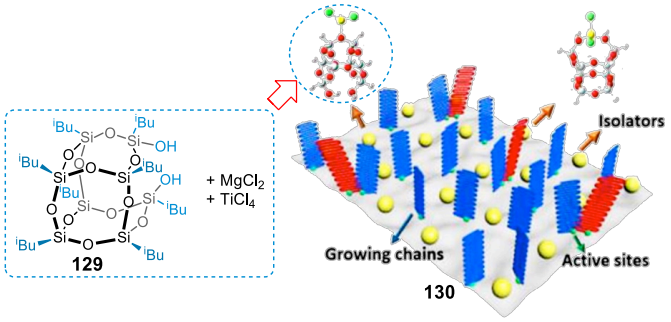

Fig. 24 POSS modified Ziegler-Natta catalyst **130** for the synthesis of weakly entangled PE. Adapted from Ref. 145. Copyright 2018, Elsevier Inc.

POSS nanostructures **129** were adsorbed on methylaluminoxane-activated silica for the immobilization of fluorinated bis(phenoxyimine)Ti complexes **131** (FI) acting as catalyst in the ethylene polymerization (**Fig. 25**).[146] In this study, POSS nanostructures were characterized as horizontal spacers isolating the active sites and hindering the chain overlap in polymerization. The resulting heterogeneous catalytic system FI/POSS/SiO_2 **132** displayed good activity in the synthesis of weakly entangled polyethylene. In particular, ethylene polymerization over FI/POSS/SiO_2 catalytic system (Al/Ti = 1100) was carried out in toluene, under 10 bar of ethylene pressure, for 30 min at 30 °C. The optimal POSS loading was found to be 10 wt% for the surface saturation and catalytic performance reaching a productivity of 16.3 $kg_{PE}\ g_{Ti}^{-1}\ h^{-1}$ and PE with molecular weight M_w of $2.0{\cdot}10^6$ $g{\cdot}mol^{-1}$ and MWD of 2.4. It is worth to mention that the catalytic system FI/POSS/SiO_2 **132** exhibited a catalytic activity four times higher than that over the FI/SiO_2 reference and close to that of the homogenous benchmark. The ultra-high molecular weight polyethylene showed a weakly entangled state with high crystallinity (80.7%) and a large fraction of monoclinic phase (15.8%). In 2018, Li *et al.* made a more detailed study on an analogous hybrid system based on Ti complex **131** immobilized onto POSS modified silica.[147] In this work, the authors focused on the evolution of polymer chains entanglements based on the fragmentation of catalytic particles. This fragmentation took place in a confined reaction environment established by POSS nanoaggregates. The polymerization of ethylene was run in toluene, under 10 bar of ethylene pressure at 30 °C. After 30 min of reaction, the catalytic productivity was 158.8 $kg_{PE}\ g_{Ti}^{-1}\ h^{-1}$ and PE molecular weight of $2.0{\cdot}10^6$ $g{\cdot}mol^{-1}$ (MWD = 2.4).

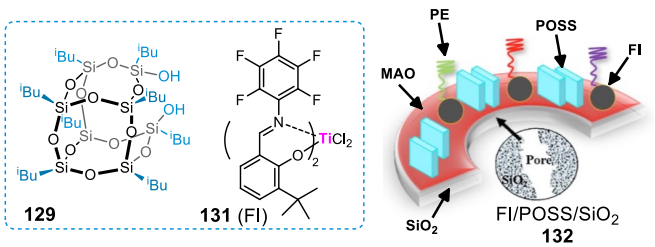

Fig. 25 Catalyst **131** immobilized on POSS modified silica. Adapted from Ref. 146. Creative Commons Attribution 3.0 License.

In 2018, Zeng *et al.* reported a series of POSS supported Cr (III) and Cr(IV) complexes as Phillips type model catalysts in ethylene polymerization to mimic the heterogeneous surface of SiO_2.[148] Chromium silsesquioxanes complexes **133a** and **133b** with bipodal structures were prepared to study the effect of POSS nanocages and chromium oxidation state on the outcoming of ethylene polymerization process (**Fig. 26**). Upon activation with tri-*n*-octylaluminum or butylated hydroxytoluene (BHT) modified triisobutylaluminum (TIBA), all the silsesquioxane-supported chromium catalysts displayed moderate activities (50-261 g_{PE} $g_{Cr}^{-1}\cdot h^{-1}$) for ethylene polymerization, producing polyethylene (PE) with M_w up to $1.9\cdot10^6$ $g\cdot mol^{-1}$ and a bimodal molecular weight distribution. Ethylene polymerization was carried out at 0.5 MPa of ethylene pressure, in heptane as a solvent, at different temperatures (50-60 °C). The obtained results evidenced the importance of the Cr oxidation state on the catalytic performance. In particular, POSS supported Cr(VI) **133b** catalysts showed much higher activity than that of POSS-supported Cr(III) **133a**. On the other hand, both **133a** and **133b** led to the production of polyethylene with lower polymerization activity than analogous Cr-complexes supported onto SiO_2 or open cage POSS nanostructures endowed with silanol moieties. This behavior suggested that the presence of silanol group in the coordination environment of chromium center plays a key role in the obtained molecular weight of polyethylene.

Hong *et al.* developed a wide series of POSS nanohybrids modified with bis(diphenylphosphino)amine (PNP) ligands **134** able to form chromium (III) complexes for catalytic ethylene trimerization and tetramerization (**Scheme 32**).[149] The proposed ligand-based catalytic systems (15 examples) exhibited high solvent tolerance and thermal stability. When an aryl group in the ligand contained a *para* substituent (-R), the catalytic activity was higher than that of the analogous ligand with a *meta* substituent. Furthermore, ligands bearing *ortho* substituents allowed to higher selectivity. The best results were achieved with the *ortho*-F-substituted aryl phosphine ligand in terms of thermal tolerance, whereas the *ortho*-OCF_3-substituted ligand displayed an outstanding catalytic activity up to 2287 $kg_{oligomers}$ g_{Cr}^{-1} h^{-1} at 45 °C, 30 bar of ethylene, after 15 min, in the presence of 500 equiv. of mMAO-3A.

Mixtures of POSS with T_8, T_9, and T_{10} nanocaged structures (**135-137**), depicted in **Fig. 27**, were adsorbed onto silica surface in order to be used as support for $(n\text{-BuCp})_2ZrCl_2$ pre-catalytic species.[150, 151]

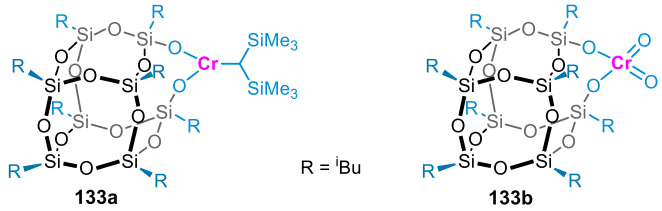

Fig. 26 Cr-POSS complexes **133a-b** for ethylene polymerization.

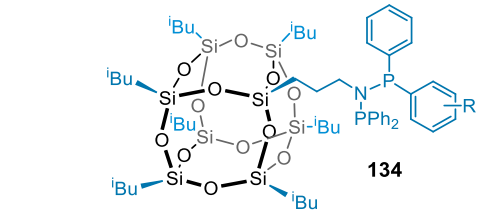

Scheme 32 Ethylene oligomerization catalytic systems based on POSS-PNP ligands **134** for Cr(III) complexes.

Such nanostructures acted as horizontal spacers improving the catalytic activity for ethylene polymerization by comparison with metallocene supported on an unmodified silica. The catalytic activity toward ethylene polymerization was evaluated in the presence of MAO (Al/Zr = 1420) after 30 min of reaction at 2 bar of ethylene pressure and 60 °C. A 10 wt% POSS modified silica, containing 0.88 wt% Zr, led to the highest productivity value of 117.8 kg_{PE} g_{Zr}^{-1} h^{-1} (M_w= $3.4\cdot10^5$ $g\cdot mol^{-1}$). This result proved to be close to that collected under homogeneous conditions, namely 134.8 kg_{PE} g_{Zr}^{-1} h^{-1} (M_w= $1.6\cdot10^5$ $g\cdot mol^{-1}$).

POSS units modified with Pd-diimine complex **140** were prepared and used as catalysts for the synthesis of polyethylene chains containing an end-tethered POSS nanocage by ethylene "living" polymerization **141**.[152] As showed in **Scheme 33**, catalyst **140** was synthesized by reaction of acryloisobutyl-POSS **139** with Pd-diimine complex **138** to form a six-membered chelate structure. Catalyst **140** was tested in chlorobenzene at 5 °C under 27.5 bar of ethylene pressure. The growing polyethylene chains were quenched with Et_3SiH to cleave the Pd–alkyl bond to release tadpole-like telechelic PEs containing a saturated group at one end and a POSS unit at the other end. In this process, the authors considered POSS nanostructures as homogeneous model supports for the Pd metal center in order to further developed the surface initiated ''living'' ethylene polymerization technique for the synthesis of PE brushes covalently bound on heterogeneous silica particles.[153]

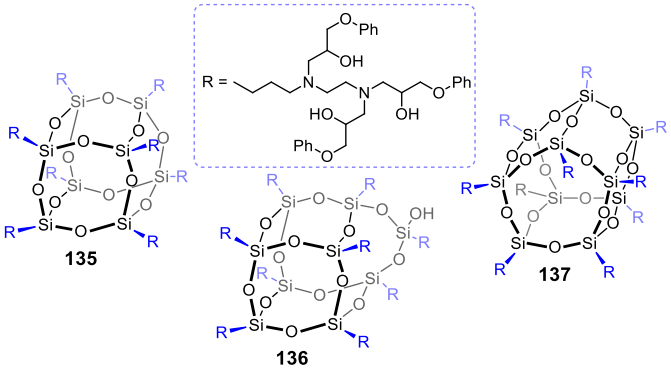

Fig. 27 T_8-T_{10} POSS nanocages **135-137** as horizontal spacers for metallocene supported silica catalysts.

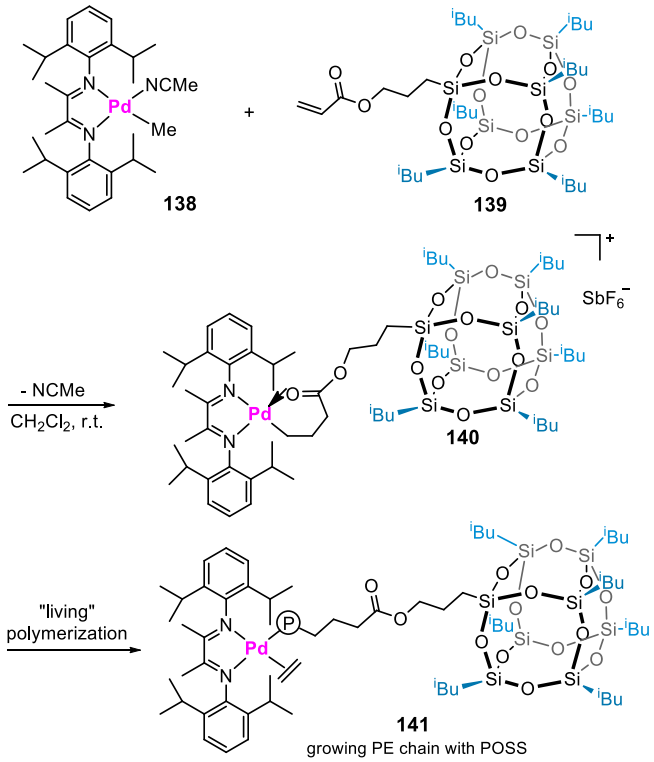

Scheme 33 POSS-supported Pd-diimine complex for ethylene "living" polymerization **141**.

The intercalation of cubic POSS in montmorillonite nanoclays allowed obtaining novel pillared structures for catalytic applications. [154, 155] Among them, porous aminopropylisooctyl POSS modified montmorillonite clay complexes (POSS-Mts) were used as Sn-catalyst supports to initiate the ring-opening polymerization of cyclic butylene terephthalate oligomers (CBT).[154] POSS-Mts hybrids with large interlayer distance and specific surface area were prepared *via* ion-exchange reaction followed by freeze-drying procedure. The specific morphology of POSS-Mts was influenced by the POSS concentration, pH of the suspension and drying procedure. The POSS-Mt supported catalyst resulted able to allow initiation and reinforcement of CBT at the same time leading to suitable nanocomposites for medical devices due to the biocompatible and thermal stability of POSS.

In 2018, POSS nanocages containing sulfonic acid groups **141** were employed as metal-free catalysts for the production of polycaprolactone (PCL) at 60 °C without using any co-catalysts and solvents (**Scheme 34**).[156] The formation of alkyl sulfonic acid moieties on POSS molecule was achieved *via* oxidation reaction from the thioester precursor. Catalyst **141** was tested at 2.5 wt% as heterogeneous system in the ring-opening polymerizations (ROP) of ε-caprolactone affording PCL in quantitative yield. Upon completion of the reaction, the polymer was dissolved in dichloromethane and the suspension of insoluble POSS catalyst was easily removed by filtration. As the loading of POSS was increased (from 2.5 up to 20.0 wt% in ε-caprolactone monomer), number average molecular weight linearly increased (M_n range: 4.0-12.4 kDa, PDI range: 1.4-1.7). Catalyst **141** was used also in the transesterification of some β-ketoesters at 3.3 mol%, in toluene at 110 °C for 2 h. However, after three consecutive reuses of **141**, a loss of the catalytic activity was observed with a decreased yield from 82% down to 47%.

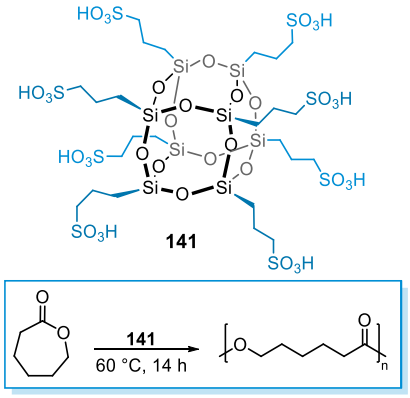

Scheme 34 POSS bearing sulfonic acid groups **141** for the synthesis of PCL.

Concluding remarks and perspectives

In this Review, we surveyed the development of POSS-based hybrids as promising catalysts for a broad spectrum of processes including oxidative and reductive reactions, C–C bond formation, carbon dioxide conversion, click reactions, and alkene polymerizations. POSS nanocages found application as templating systems for the synthesis of ionic porous polymers with enhanced performances compared to analogous POSS-free materials. The use of POSS molecules as nano-building blocks provides new avenues for the synthesis of heterogeneous catalysts thorough a ''Lego-like'' chemistry. Moreover, POSS nanostructures can be extensively studied as molecular model for the design of novel heterogeneous materials.[29] POSS nanohybrids have been used as stabilizing support for metal nanoparticles, as suitable ligand for organometallic complexes, and as host nanostructures for single sites metal species. As evidences by some studies,[77, 80, 106] the chemical modification of POSS nanocages enable the local concentration of catalytic active sites in a confined reaction environment showing better performances by comparison with both analogous unsupported active sites and heterogeneous catalysts grafted onto different supports. In other works, POSS-based catalysts showed higher activity than commercial catalysts for alcohol oxidations,[65] formic acid electooxidation,[66, 67] hydrosilylation reactions,[122] and ethylene polymerization.[144] Continuous flow nanofiltration reactor setup was employed for POSS ligands able to generate, *in situ*, rhodium catalysts for the hydroformylation of 1-octene[98] and olefins metathesis.[101] From the above, POSS nanostructures may find application in future studies of flow- or continuous-synthesis systems.

The implementation of POSS applications in the field of catalysis can be achieved by considering emerging research interests as the chemistry of mussel-inspired polydopamine (PDA) hybrids. Very recently, the combined use of POSS and PDA led to novel nanocomposites with peculiar surface properties. POSS-PDA hybrid coatings have been applied on Kevlar cloth,[157] PE

separators,[158] multiwalled carbon nanotubes,[159] carbon fibers,[160] graphene oxide,[161] bridged polysilsesquioxane nanoparticles,[162] and polyacrylonitrile.[163] Moreover, polydopamine-modified POSS were incorporated as acid-base nano-filler to address the trade-off between conductivity and stabilities for proton exchange membranes.[164] Over the past decades, PDA-based materials found a prolific use as catalysts able to incorporate enzymes, to stabilize metal particles and oxides, and to form complexes with metal ions.[165] The properties of both PDA and POSS nanostructures could allow novel performing catalytic materials processed into ad-layer, thin and robust coatings and films, hollow capsules, nanofibers, membranes, nanoparticles, and core-shell structures as well.[126] Furthermore, POSS-based catalysts could be applied for the biomass valorization. In particular, new catalytic systems could be developed through the functionalization of POSS nanohybrids with acid, base or redox active sites in order to test the obtained materials as multifunctional catalysts in cascade biomass processes.[166] By virtues of their highly tuneable properties combined with a high mechanical stability, POSS nanostructures bring promising perspectives in the field of heterogeneous catalysis paving the way to new libraries of hybrid catalysts.

Conflicts of interest

There are no conflicts to declare.

Acknowledgements

This work was financially supported by the University of Palermo and was carried out in the frame of the PRIN2017-2017YJMPZN project.

References

1. P. D. Lickiss and F. Rataboul, in *Adv. Organomet. Chem.*, eds. A. F. Hill and M. J. Fink, Academic Press, 2008, vol. 57, pp. 1-116.
2. D. B. Cordes, P. D. Lickiss and F. Rataboul, *Chem. Rev.*, 2010, **110**, 2081-2173.
3. H. Zhou, Q. Ye and J. Xu, *Mater. Chem. Front.*, 2017, **1**, 212-230.
4. F. Dong, L. Lu and C.-S. Ha, *Macromol. Chem. Phys.*, 2019, **220**, 1800324.
5. R. Müller, R. Köhne and S. Sliwinski, *J. Prakt. Chem.*, 1959, **9**, 71-74.
6. D. B. Cordes and P. D. Lickiss, in *Applications of Polyhedral Oligomeric Silsesquioxanes*, ed. C. Hartmann-Thompson, Springer Netherlands, Dordrecht, 2011, DOI: 10.1007/978-90-481-3787-9_2, pp. 47-133.
7. Q. Ye, H. Zhou and J. Xu, *Chem. Asian J.*, 2016, **11**, 1322-1337.
8. K. Tanaka and Y. Chujo, *J. Mater. Chem.*, 2012, **22**, 1733-1746.
9. F. Chen, F. Lin, Q. Zhang, R. Cai, Y. Wu and X. Ma, *Macromol. Rapid Commun.*, 2019, **40**, 1900101.
10. N. Ahmed, H. Fan, P. Dubois, X. Zhang, S. Fahad, T. Aziz and J. Wan, *J. Mater. Chem. A*, 2019, **7**, 21577-21604.
11. K. Pielichowski, J. Njuguna, B. Janowski and J. Pielichowski, in *Supramolecular Polymers Polymeric Betains Oligomers*, Springer Berlin Heidelberg, Berlin, Heidelberg, 2006, DOI: 10.1007/12_077, pp. 225-296.
12. S.-W. Kuo and F.-C. Chang, *Prog. Polym. Sci.*, 2011, **36**, 1649-1696.
13. W. Zhang and A. H. E. Müller, *Prog. Polym. Sci.*, 2013, **38**, 1121-1162.
14. A. Kausar, *Polym. Plast. Technol. Eng.*, 2017, **56**, 1401-1420.
15. G. M. Mohamed and W. S. Kuo, *Polymers*, 2018, **11**.
16. W. Zhang, G. Camino and R. Yang, *Prog. Polym. Sci.*, 2017, **67**, 77-125.
17. Z. Li, J. Kong, F. Wang and C. He, *J. Mater. Chem. C*, 2017, **5**, 5283-5298.
18. H. Ghanbari, B. G. Cousins and A. M. Seifalian, *Macromol. Rapid Commun.*, 2011, **32**, 1032-1046.
19. Z. Zhou and Z.-R. Lu, *Nanomedicine*, 2014, **9**, 2387-2401.
20. Q. Yang, L. Li, W. Sun, Z. Zhou and Y. Huang, *ACS Appl. Mater. Interfaces*, 2016, **8**, 13251-13261.
21. M. Chen, Y. Zhang, Q. Xie, W. Zhang, X. Pan, P. Gu, H. Zhou, Y. Gao, A. Walther and X. Fan, *ACS Biomater. Sci. Eng.*, 2019, **5**, 4612-4623.
22. H.-B. He, B. Li, J.-P. Dong, Y.-Y. Lei, T.-L. Wang, Q.-W. Yu, Y.-Q. Feng and Y.-B. Sun, *ACS Appl. Mater. Interfaces*, 2013, **5**, 8058-8066.
23. H. Liu, R. Sun, S. Feng, D. Wang and H. Liu, *Chem. Eng. J.*, 2019, **359**, 436-445.
24. X. Yang and H. Liu, *Chem. Eur. J.*, 2018, **24**, 13504-13511.
25. X. Wang, R. Peng, H. He, X. Yan, S. Zhu, H. Zhao, D. Deng, Y. Qiongwei, Y. Lei and L. Luo, *Colloids Surf. A Physicochem. Eng. Asp.*, 2018, **550**, 1-8.
26. H. Liu, Z. Chen, S. Feng, D. Wang and H. Liu, *Polymers*, 2019, **11**.
27. A. C. Kucuk and O. A. Urucu, *React. Funct. Polym.*, 2019, **140**, 22-30.
28. S. Bandehali, F. Parvizian, A. R. Moghadassi and S. M. Hosseini, *J. Polym. Res.*, 2019, **26**, 211.
29. E. A. Quadrelli and J.-M. Basset, *Coord. Chem. Rev.*, 2010, **254**, 707-728.
30. P. P. Pescarmona, C. Aprile and S. Swaminathan, in *New and Future Developments in Catalysis*, ed. S. L. Suib, Elsevier, Amsterdam, 2013, DOI: https://doi.org/10.1016/B978-0-444-53876-5.00018-0, pp. 385-422.
31. C. Copéret, A. Comas-Vives, M. P. Conley, D. P. Estes, A. Fedorov, V. Mougel, H. Nagae, F. Núñez-Zarur and P. A. Zhizhko, *Chem. Rev.*, 2016, **116**, 323-421.
32. P. Guillo, M. I. Lipschutz, M. E. Fasulo and T. D. Tilley, *ACS Catal.*, 2017, **7**, 2303-2312.
33. M. Nowotny, T. Maschmeyer, B. F. G. Johnson, P. Lahuerta, J. M. Thomas and J. E. Davies, *Angew. Chem. Int. Ed.*, 2001, **40**, 955-958.
34. K. Wada, M. Nakashita, A. Yamanoto, H. Wada and T.-a. Mitsudo, *Chem. Lett.*, 1997, **26**, 1209-1210.
35. K. Wada, M. Nakashita, A. Yamamoto, H. Wada and T. Mitsudo, *Res. Chem. Intermed.*, 1998, **24**, 515-527.
36. K. Wada, M. Nakashita and T. Mitsudo, *Chem. Commun.*, 1998, DOI: 10.1039/A707173F, 133-134.

37. G. Chen, Y. Zhou, X. Wang, J. Li, S. Xue, Y. Liu, Q. Wang and J. Wang, *Sci. Rep.*, 2015, **5**, 11236.
38. H. C. L. Abbenhuis, S. Krijnen and R. A. van Santen, *Chem. Commun.*, 1997, DOI: 10.1039/A607935K, 331-332.
39. F. J. Feher, T. A. Budzichowski, K. Rahimian and J. W. Ziller, *J. Am. Chem. Soc.*, 1992, **114**, 3859-3866.
40. S. Krijnen, H. C. L. Abbenhuis, R. W. J. M. Hanssen, J. H. C. van Hooff and R. A. van Santen, *Angew. Chem. Int. Ed.*, 1998, **37**, 356-358.
41. S. Krijnen, B. L. Mojet, H. C. L. Abbenhuis, J. H. C. Van Hooff and R. A. Van Santen, *Phys. Chem. Chem. Phys.*, 1999, **1**, 361-365.
42. M. Crocker, R. H. M. Herold, M. Crocker and A. Guy Orpen, *Chem. Commun.*, 1997, DOI: 10.1039/A704969B, 2411-2412.
43. P. P. Pescarmona, J. C. van der Waal, I. E. Maxwell and T. Maschmeyer, *Angew. Chem. Int. Ed.*, 2001, **40**, 740-743.
44. P. P. Pescarmona, T. Maschmeyer and J. C. Van Der Waal, *Chem. Eng. Commun.*, 2004, **191**, 68-74.
45. M. D. Skowronska-Ptasinska, M. L. W. Vorstenbosch, R. A. van Santen and H. C. L. Abbenhuis, *Angew. Chem. Int. Ed.*, 2002, **41**, 637-639.
46. L. Zhang, H. C. L. Abbenhuis, G. Gerritsen, N. N. Bhriain, P. C. M. M. Magusin, B. Mezari, W. Han, R. A. van Santen, Q. Yang and C. Li, *Chem. Eur. J.*, 2007, **13**, 1210-1221.
47. F. Carniato, C. Bisio, E. Boccaleri, M. Guidotti, E. Gavrilova and L. Marchese, *Chem. Eur. J.*, 2008, **14**, 8098-8101.
48. F. Carniato, C. Bisio, L. Sordelli, E. Gavrilova and M. Guidotti, *Inorg. Chim. Acta*, 2012, **380**, 244-251.
49. S. Sakugawa, K. Wada and M. Inoue, *J. Catal.*, 2010, **275**, 280-287.
50. K. Wada, S. Sakugawa and M. Inoue, *Chem. Commun.*, 2012, **48**, 7991-7993.
51. K. Wada, K. Hirabayashi, N. Watanabe, S. Yamamoto, T. Kondo, T.-a. Mitsudo and M. Inoue, *Top. Catal.*, 2009, **52**, 693-698.
52. E. H. Aish, M. Crocker and F. T. Ladipo, *J. Catal.*, 2010, **273**, 66-72.
53. I. V. Soares, E. G. Vieira, N. L. D. Filho, A. C. Bastos, N. C. da Silva, E. F. Garcia and L. J. A. Lima, *Chem. Eng. J.*, 2013, **218**, 405-414.
54. M. Vasconcellos Dias, M. S. Saraiva, P. Ferreira and M. J. Calhorda, *Organometallics*, 2015, **34**, 1465-1478.
55. E. G. Vieira, A. G. Dal-Bó, T. E. A. Frizon and N. L. Dias Filho, *J. Organomet. Chem.*, 2017, **834**, 73-82.
56. E. G. Vieira, R. O. Silva, E. F. Junior and N. L. Dias Filho, *Appl. Organomet. Chem.*, 2017, **31**, e3722.
57. E. G. Vieira, R. O. Silva, A. G. Dal-Bó, T. E. A. Frizon and N. L. D. Filho, *New J. Chem.*, 2016, **40**, 9403-9414.
58. E. G. Vieira and N. L. Dias Filho, *Mater. Chem. Phys.*, 2017, **201**, 262-270.
59. Y. Leng, J. Liu, C. Zhang and P. Jiang, *Catal. Sci. Technol.*, 2014, **4**, 997-1004.
60. Y. Leng, J. Liu, P. Jiang and J. Wang, *ACS Sustainable Chem. Eng.*, 2015, **3**, 170-176.
61. Y. Leng, J. Zhao, P. Jiang and J. Wang, *RSC Adv.*, 2015, **5**, 17709-17715.
62. J. Zhao, Y. Leng, P. Jiang, J. Wang and C. Zhang, *New J. Chem.*, 2016, **40**, 1022-1028.
63. K. Wada, K. Yano, T. Kondo and T.-a. Mitsudo, *Catal. Lett.*, 2006, **112**, 63-67.
64. P. Sangtrirutnugul, T. Chaiprasert, W. Hunsiri, T. Jitjaroendee, P. Songkhum, K. Laohhasurayotin, T. Osotchan and V. Ervithayasuporn, *ACS Appl. Mater. Interfaces*, 2017, **9**, 12812-12822.
65. S. Li, Z. Chen, X. Ling, J. Cao, Q. Wang, Y. Zhou and J. Wang, *Appl. Surf. Sci.*, 2019, **496**, 143650.
66. Y. Li, F. Hao, Y. Wang, Y. Zhang, C. Ge and T. Lu, *Electrochim. Acta*, 2014, **133**, 302-307.
67. T. Chen, C. Ge, Y. Zhang, Q. Zhao, F. Hao and N. Bao, *Int. J. Hydrogen Energy*, 2015, **40**, 4548-4557.
68. Q. Zhao, C. Ge, Y. Cai, Q. Qiao and X. Jia, *J. Colloid Interface Sci.*, 2018, **514**, 425-432.
69. K. Qian, F. Hao, S. Wei, Y. Wang, C. Ge, P. Chen and Y. Zhang, *J. Solid State Electrochem.*, 2017, **21**, 297-304.
70. P. P. Pescarmona, A. F. Masters, J. C. van der Waal and T. Maschmeyer, *J. Mol. Catal. A: Chem.*, 2004, **220**, 37-42.
71. M. T. Hay, S. J. Geib and D. A. Pettner, *Polyhedron*, 2009, **28**, 2183-2186.
72. D. Wang and E. Mejía, *ChemistrySelect*, 2017, **2**, 3381-3387.
73. C.-H. Lu and F.-C. Chang, *ACS Catal.*, 2011, **1**, 481-488.
74. P. Scholder and I. Nischang, *Catal. Sci. Technol.*, 2015, **5**, 3917-3921.
75. V. Ervithayasuporn, K. Kwanplod, J. Boonmak, S. Youngme and P. Sangtrirutnugul, *J. Catal.*, 2015, **332**, 62-69.
76. C. Zhang, Y. Leng, P. Jiang and D. Lu, *RSC Adv.*, 2016, **6**, 57183-57189.
77. L. A. Bivona, F. Giacalone, E. Carbonell, M. Gruttadauria and C. Aprile, *ChemCatChem*, 2016, **8**, 1685-1691.
78. S. Mohapatra, T. Chaiprasert, R. Sodkhomkhum, R. Kunthom, S. Hanprasit, P. Sangtrirutnugul and V. Ervithayasuporn, *ChemistrySelect*, 2016, **1**, 5353-5357.
79. V. Somjit, M. Wong Chi Man, A. Ouali, P. Sangtrirutnugul and V. Ervithayasuporn, *ChemistrySelect*, 2018, **3**, 753-759.
80. C. Calabrese, V. Campisciano, F. Siragusa, L. F. Liotta, C. Aprile, M. Gruttadauria and F. Giacalone, *Adv. Synth. Catal.*, 2019, **361**, 3758-3767.
81. S. Sadjadi, M. Malmir, M. M. Heravi and M. Raja, *Int. J. Biol. Macromol.*, 2019, **128**, 638-647.
82. W. Zheng, C. Lu, G. Yang, Z. Chen and J. Nie, *Catal. Commun.*, 2015, **62**, 34-38.
83. P. Szcześniak, O. Staszewska-Krajewska, B. Furman and J. Mlynarski, *Tetrahedron: Asymmetry*, 2017, **28**, 1765-1773.
84. T. Luanphaisarnnont, S. Hanprasit, V. Somjit and V. Ervithayasuporn, *Catal. Lett.*, 2018, **148**, 779-786.
85. T. Ishii, S. Fujioka, Y. Sekiguchi and H. Kotsuki, *J. Am. Chem. Soc.*, 2004, **126**, 9558-9559.
86. P. Li, L. Wang, Y. Zhang and G. Wang, *Tetrahedron*, 2008, **64**, 7633-7638.
87. U. Díaz, T. García, A. Velty and A. Corma, *Chem. Eur. J.*, 2012, **18**, 8659-8672.
88. J. Safaei-Ghomi, S. H. Nazemzadeh and H. Shahbazi-Alavi, *Catal. Commun.*, 2016, **86**, 14-18.
89. J. Safaei-Ghomi, S. H. Nazemzadeh and H. Shahbazi-Alavi, *Appl. Organomet. Chem.*, 2016, **30**, 911-916.
90. Y. Zhou, G. Yang, C. Lu, J. Nie, Z. Chen and J. Ren, *Catal. Commun.*, 2016, **75**, 23-27.
91. L. c. Ropartz, R. E. Morris, G. P. Schwarz, D. F. Foster and D. J. Cole-Hamilton, *Inorg. Chem. Commun.*, 2000, **3**, 714-717.
92. L. Ropartz, R. E. Morris, D. F. Foster and D. J. Cole-Hamilton, *Chem. Commun.*, 2001, DOI: 10.1039/B009574P, 361-362.

93. L. Ropartz, K. J. Haxton, D. F. Foster, R. E. Morris, A. M. Z. Slawin and D. J. Cole-Hamilton, *J. Chem. Soc., Dalton Trans.*, 2002, DOI: 10.1039/B206597E, 4323-4334.
94. L. c. Ropartz, R. E. Morris, D. F. Foster and D. J. Cole-Hamilton, *J. Mol. Catal. A: Chem.*, 2002, **182-183**, 99-105.
95. L. Ropartz, D. F. Foster, R. E. Morris, A. M. Z. Slawin and D. J. Cole-Hamilton, *J. Chem. Soc., Dalton Trans.*, 2002, DOI: 10.1039/B200303A, 1997-2008.
96. N. R. Vautravers and D. J. Cole-Hamilton, *Chem. Commun.*, 2009, DOI: 10.1039/B814582B, 92-94.
97. J. I. van der Vlugt, J. Ackerstaff, T. W. Dijkstra, A. M. Mills, H. Kooijman, A. L. Spek, A. Meetsma, H. C. L. Abbenhuis and D. Vogt, *Adv. Synth. Catal.*, 2004, **346**, 399-412.
98. M. Janssen, J. Wilting, C. Müller and D. Vogt, *Angew. Chem. Int. Ed.*, 2010, **49**, 7738-7741.
99. F. J. Feher and T. L. Tajima, *J. Am. Chem. Soc.*, 1994, **116**, 2145-2146.
100. H. M. Cho, H. Weissman, S. R. Wilson and J. S. Moore, *J. Am. Chem. Soc.*, 2006, **128**, 14742-14743.
101. A. Kajetanowicz, J. Czaban, G. R. Krishnan, M. Malińska, K. Woźniak, H. Siddique, L. G. Peeva, A. G. Livingston and K. Grela, *ChemSusChem*, 2013, **6**, 182-192.
102. A. Falk, J. M. Dreimann and D. Vogt, *ACS Sustainable Chem. Eng.*, 2018, **6**, 7221-7226.
103. C. Calabrese, F. Giacalone and C. Aprile, *Catalysts*, 2019, **9**.
104. A. J. Kamphuis, F. Picchioni and P. P. Pescarmona, *Green Chem.*, 2019, **21**, 406-448.
105. V. Campisciano, C. Calabrese, F. Giacalone, C. Aprile, P. Lo Meo and M. Gruttadauria, *J. CO2 Util.*, 2020, **38**, 132-140.
106. L. A. Bivona, O. Fichera, L. Fusaro, F. Giacalone, M. Buaki-Sogo, M. Gruttadauria and C. Aprile, *Catal. Sci. Technol.*, 2015, **5**, 5000-5007.
107. J. H. Lee, A. S. Lee, J.-C. Lee, S. M. Hong, S. S. Hwang and C. M. Koo, *ACS Appl. Mater. Interfaces*, 2017, **9**, 3616-3623.
108. X. Meng, Y. Liu, S. Wang, J. Du, Y. Ye, X. Song and Z. Liang, *ACS Appl. Polym. Mater.*, 2020, **2**, 189-197.
109. C. Calabrese, L. F. Liotta, F. Giacalone, M. Gruttadauria and C. Aprile, *ChemCatChem*, 2019, **11**, 560-567.
110. C. Calabrese, L. Fusaro, L. F. Liotta, F. Giacalone, A. Comès, V. Campisciano, C. Aprile and M. Gruttadauria, *ChemPlusChem*, 2019, **84**, 1536-1543.
111. G. Chen, X. Huang, Y. Zhang, M. Sun, J. Shen, R. Huang, M. Tong, Z. Long and X. Wang, *Chem. Commun.*, 2018, **54**, 12174-12177.
112. Y. Zhang, K. Liu, L. Wu, H. Zhong, N. Luo, Y. Zhu, M. Tong, Z. Long and G. Chen, *ACS Sustainable Chem. Eng.*, 2019, **7**, 16907-16916.
113. G. Chen, Y. Zhang, J. Xu, X. Liu, K. Liu, M. Tong and Z. Long, *Chem. Eng. J.*, 2020, **381**, 122765.
114. D. Lu, J. Zhao, Y. Leng, P. Jiang and C. Zhang, *Catal. Commun.*, 2016, **83**, 27-30.
115. Y. Leng, J. Zhao, P. Jiang and D. Lu, *Catal. Sci. Technol.*, 2016, **6**, 875-881.
116. S. E. Létant, J. Herberg, L. N. Dinh, R. S. Maxwell, R. L. Simpson and A. P. Saab, *Catal. Commun.*, 2007, **8**, 2137-2142.
117. X. Li, Y. Du, J. Dai, X. Wang and P. Yang, *Catal. Lett.*, 2007, **118**, 151-158.
118. W. Zhou, J. Wang, C. Wang, Y. Du, J. Xu and P. Yang, *Mater. Chem. Phys.*, 2010, **122**, 10-14.
119. E. S. Cozza, V. Bruzzo, F. Carniato, E. Marsano and O. Monticelli, *ACS Appl. Mater. Interfaces*, 2012, **4**, 604-607.
120. L. Gardella, A. Basso, M. Prato and O. Monticelli, *ACS Appl. Mater. Interfaces*, 2013, **5**, 7688-7692.
121. S. Tang, R. Jin, H. Zhang, H. Yao, J. Zhuang, G. Liu and H. Li, *Chem. Commun.*, 2012, **48**, 6286-6288.
122. Z. Liu, S. Ma, L. Chen, J. Xu, J. Ou and M. Ye, *Mater. Chem. Front.*, 2019, **3**, 851-859.
123. P. Scholder, M. Hafner, A. W. Hassel and I. Nischang, *Eur. J. Inorg. Chem.*, 2016, **2016**, 951-955.
124. F. Kazeminava, N. Arsalani and A. Akbari, *Appl. Organomet. Chem.*, 2018, **32**, e4359.
125. A. Akbari, A. Naderahmadian and B. Eftekhari-Sis, *Polyhedron*, 2019, **171**, 228-236.
126. G. Kibar and D. Ş. Ö. Dinç, *J. Environ. Chem. Eng.*, 2019, **7**, 103435.
127. S. Xia, Y. Yang, W. Zhu and C. Lü, *Colloids Surf. A Physicochem. Eng. Asp.*, 2020, **585**, 124110.
128. A. Akbari, N. Arsalani, M. Amini and E. Jabbari, *J. Mol. Catal. A: Chem.*, 2016, **414**, 47-54.
129. R. Duchateau, *Chem. Rev.*, 2002, **102**, 3525-3542.
130. F. J. Feher, J. F. Walzer and R. L. Blanski, *J. Am. Chem. Soc.*, 1991, **113**, 3618-3619.
131. F. J. Feher and J. F. Walzer, *Inorg. Chem.*, 1991, **30**, 1689-1694.
132. F. J. Feher and R. L. Blanski, *J. Am. Chem. Soc.*, 1992, **114**, 5886-5887.
133. M. Białek, M. Pochwała, A. Franczyk, K. Czaja and B. Marciniec, *Polym. Int.*, 2017, **66**, 960-967.
134. R. Duchateau, H. C. L. Abbenhuis, R. A. van Santen, S. K. H. Thiele and M. F. H. van Tol, *Organometallics*, 1998, **17**, 5222-5224.
135. R. Duchateau, U. Cremer, R. J. Harmsen, S. I. Mohamud, H. C. L. Abbenhuis, R. A. van Santen, A. Meetsma, S. K. H. Thiele, M. F. H. van Tol and M. Kranenburg, *Organometallics*, 1999, **18**, 5447-5459.
136. R. Duchateau, H. C. L. Abbenhuis, R. A. van Santen, A. Meetsma, S. K. H. Thiele and M. F. H. van Tol, *Organometallics*, 1998, **17**, 5663-5673.
137. J. R. Severn, R. Duchateau, R. A. van Santen, D. D. Ellis and A. L. Spek, *Organometallics*, 2002, **21**, 4-6.
138. J. R. Severn, R. Duchateau, R. A. van Santen, D. D. Ellis, A. L. Spek and G. P. A. Yap, *Dalton Trans.*, 2003, DOI: 10.1039/B300698K, 2293-2302.
139. R. Duchateau, R. A. van Santen and G. P. A. Yap, *Organometallics*, 2000, **19**, 809-816.
140. A. M. Mehta, G. L. Tembe, P. A. Parikh and G. N. Mehta, *React. Kinet. Mech. Catal.*, 2011, **104**, 369-375.
141. A. Mehta, G. Tembe, M. Białek, P. Parikh and G. Mehta, *Polym. Adv. Technol.*, 2013, **24**, 441-445.
142. A. Mehta, G. Tembe, M. Białek, P. Parikh and G. Mehta, *J. Mol. Catal. A: Chem.*, 2012, **361-362**, 17-28.
143. V. Varga, T. Hodík, M. Lamač, M. Horáček, A. Zukal, N. Žilková, W. O. Parker and J. Pinkas, *J. Organomet. Chem.*, 2015, **777**, 57-66.
144. J.-C. Liu, *Chem. Commun.*, 1996, DOI: 10.1039/CC9960001109, 1109-1110.
145. W. Li, L. Hui, B. Xue, C. Dong, Y. Chen, L. Hou, B. Jiang, J. Wang and Y. Yang, *J. Catal.*, 2018, **360**, 145-151.
146. W. Li, H. Yang, J. Zhang, J. Mu, D. Gong and X. Wang, *Chem. Commun.*, 2016, **52**, 11092-11095.
147. L. Hui, Z. Yue, H. Yang, T. Chen and W. Li, *Ind. Eng. Chem. Res.*, 2018, **57**, 9400-9406.

148. Y. Zeng, S. Liu and M. Terano, *Macromol. React. Eng.*, 2018, **12**, 1800049.
149. H. Lee and S. H. Hong, *Appl. Catal. A Gen.*, 2018, **560**, 21-27.
150. D. Bianchini, G. B. Galland, J. H. Z. dos Santos, R. J. J. Williams, D. P. Fasce, I. E. Dell'Erba, R. Quijada and M. Perez, *J. Polym. Sci., Part A: Polym. Chem.*, 2005, **43**, 5465-5476.
151. I. García-Orozco, T. Velilla, G. B. Galland, J. H. Z. dos Santos, R. J. J. Williams and R. Quijada, *J. Polym. Sci., Part A: Polym. Chem.*, 2010, **48**, 5938-5944.
152. Y. Zhang and Z. Ye, *Chem. Commun.*, 2008, DOI: 10.1039/B716900K, 1178-1180.
153. Y. Zhang and Z. Ye, *Macromolecules*, 2008, **41**, 6331-6338.
154. C. Wan, F. Zhao, X. Bao, B. Kandasubramanian and M. Duggan, *J. Phys. Chem. B*, 2008, **112**, 11915-11922.
155. G. Potsi, A. K. Ladavos, D. Petrakis, A. P. Douvalis, Y. Sanakis, M. S. Katsiotis, G. Papavassiliou, S. Alhassan, D. Gournis and P. Rudolf, *J. Colloid Interface Sci.*, 2018, **510**, 395-406.
156. R. Kunthom, T. Jaroentomeechai and V. Ervithayasuporn, *Polymer*, 2017, **108**, 173-178.
157. L. Tang, J. Dang, M. He, J. Li, J. Kong, Y. Tang and J. Gu, *Compos. Sci. Technol.*, 2019, **169**, 120-126.
158. Y. Wang, L. Shi, H. Zhou, Z. Wang, R. Li, J. Zhu, Z. Qiu, Y. Zhao, M. Zhang and S. Yuan, *Electrochim. Acta*, 2018, **259**, 386-394.
159. L. Gao, Q. Zhang, M. Zhu, X. Zhang, G. Sui and X. Yang, *Mater. Lett.*, 2016, **183**, 207-210.
160. X. Yang, H. Du, S. Li, Z. Wang and L. Shao, *ACS Sustainable Chem. Eng.*, 2018, **6**, 4412-4420.
161. S. Zhang, Y. Tang, Y. Chen, J. Zhang and Y. Wei, *Microchim. Acta*, 2020, **187**, 77.
162. S. Oh, P.-s. Kang, Y. Lee, J.-I. Lee, N.-H. Park, J.-H. Lim and K.-M. Kim, *Mol. Cryst. Liq. Cryst.*, 2019, **686**, 38-44.
163. X. You, H. Wu, Y. Su, J. Yuan, R. Zhang, Q. Yu, M. Wu, Z. Jiang and X. Cao, *J. Mater. Chem. A*, 2018, **6**, 13191-13202.
164. P. Zhang, W. Li, L. Wang, C. Gong, J. Ding, C. Huang, X. Zhang, S. Zhang, L. Wang and W. Bu, *J. Membr. Sci.*, 2020, **596**, 117734.
165. Á. Molnár, *ChemCatChem*, 2020, **n/a**, DOI: 10.1002/cctc.201902125.
166. P. Sudarsanam, R. Zhong, S. Van den Bosch, S. M. Coman, V. I. Parvulescu and B. F. Sels, *Chem. Soc. Rev.*, 2018, **47**, 8349-8402.